

Higgs boson mass and thermal wino dark matter from Starobinsky supergravity with the MSSM

Daniel Frolovsky^{a,b,c,*}, Alexander Belyaev^{d,e,†}, and Sergei V. Ketov^{c,f,g,h,‡}

^a *Institute for Theoretical Physics, Utrecht University,
Princetonplein 5, 3584 CC Utrecht, Netherlands*

^b *Dutch Institute for Emergent Phenomena, Netherlands*

^c *Department of Physics and Interdisciplinary Research Laboratory,
Tomsk State University, Tomsk 634050, Russia*

^d *School of Physics and Astronomy, University of Southampton,
Highfield, Southampton SO17 1BJ, UK*

^e *Particle Physics Department, Rutherford Appleton Laboratory,
Chilton, Didcot, Oxon OX11 0QX, UK*

^f *Department of Physics, Faculty of Science, Tokyo Metropolitan University,
1-1 Minami-ohsawa, Tokyo 192-0397, Japan*

^g *International Institute of Physics, Natal 1613,
Rio Grande do Norte 59078-970, Brazil*

^h *Kavli Institute for the Physics and Mathematics of the Universe (WPI),
The University of Tokyo Institutes for Advanced Study, Chiba 277-8583, Japan*

Abstract

We propose a framework connecting cosmic microwave background (CMB) observables with high-energy particle phenomenology, based on Starobinsky supergravity coupled to the Minimal Supersymmetric Standard Model (MSSM). Cosmic inflation and supersymmetry (SUSY) breaking occur within the hidden sector emerging from Starobinsky supergravity. The inflationary scale fixes the characteristic mass scale of the hidden sector, which determines the MSSM soft terms through gravitational mediation of SUSY breaking. The same hidden sector can also dynamically generate a high-scale μ term. The resulting MSSM spectrum fixes the high-scale threshold corrections and the boundary conditions for the renormalisation-group (RG) evolution of the Higgs quartic coupling. Three-loop RG evolution of the Higgs quartic coupling gives a Higgs boson mass consistent with the measured value within the theoretical and experimental uncertainties, thereby linking the amplitude of primordial scalar perturbations to the Higgs boson mass. With conserved R -parity, the lightest supersymmetric particle is stable, making it a compelling dark matter candidate. The observed relic abundance selects a nearly pure thermal wino with a physical mass of about 3 TeV. Its loop-induced spin-independent wino-nucleon scattering cross section lies below the current sensitivity of the LUX-ZEPLIN experiment, but within the projected reach of next-generation multi-ton liquid-xenon detectors. Electroweak radiative corrections generate a small mass splitting between the charged and neutral wino states, leading to a long-lived charged wino and the characteristic disappearing-track signature. A future 100 TeV proton collider can discover the disappearing-track signal from a 3 TeV wino or fully exclude this thermal wino dark matter scenario.

* d.frolovskiy@uu.nl, the corresponding author

† a.belyaev@soton.ac.uk

‡ ketov@tmu.ac.jp

Contents

1	Introduction	3
2	Starobinsky supergravity setup	5
3	Scalar potential, inflation and gravitino mass	8
4	Coupling of Starobinsky supergravity to MSSM	11
5	Soft MSSM parameters and RG running	13
6	Anomaly mediation of SUSY breaking and wino dark matter	18
7	Conclusion	23
A	Higgs mass uncertainties, and comparison of SusyHD and HSSUSY	25

1 Introduction

One of the outstanding problems in high-energy physics is to connect the Standard Model (SM) of particle physics with cosmological inflation in the early Universe. On the one hand, the SM is the standard theoretical framework describing strong, weak and electromagnetic interactions of elementary particles, which was tested on the electroweak (EW) scale with high precision. However, as is well known, the SM is phenomenologically and theoretically incomplete because it does not include gravity and a particle candidate for dark matter (DM), it does not explain baryon asymmetry of the Universe and non-vanishing neutrino masses as well. The SM breaks down at very high energies when approaching the Grand Unification scale, thus requiring new physics beyond the SM. On the other hand, inflation provides a window into new physics beyond the SM, which is testable due to observations of the cosmic microwave background (CMB) radiation with high precision also. Inflation eliminates conceptual shortcomings of the standard (Einstein-Friedmann) cosmology such as the horizon and flatness problems, and provides a mechanism for generation of primordial density perturbations leading to the structure formation in the Universe. Connecting inflation to the SM is also needed for explaining the origin of elementary particles during reheating after inflation.

The existing approaches to inflation and reheating are highly model-dependent, see e.g., Refs. [1–4] for a review and Refs. [5–8] for the earlier attempts to connect inflation to the SM. In this paper, we assume two main underlying concepts, namely, Starobinsky inflation [9–11] and local supersymmetry [12–14].

Starobinsky inflation can be described in two equivalent pictures known as modified gravity and scalar-tensor gravity. These pictures are related by a Weyl transformation of spacetime metric between the so-called Jordan and Einstein frames, respectively. The modified gravity picture has the higher derivatives and the hidden scalar (inflaton) degree of freedom, whereas in the Einstein frame there are no higher derivatives and inflaton is manifest but the gravitational origin of the inflaton potential is hidden. The Starobinsky model based on the modified gravity action

$$S = \int d^4x \sqrt{-g} \left(\frac{M_{\text{P}}^2}{2} R + \frac{M_{\text{P}}^2}{12m_{\text{S}}^2} R^2 \right) \quad (1)$$

is one of the most successful models of inflation, in excellent agreement with CMB observations by the Planck mission [15]. This is more than just a good fit because the Starobinsky model is simple, geometrical, ghost-free and tightly constrained, being entirely based on gravitational interactions. It explains the origin of inflaton and the approximate flatness of its scalar potential in the Einstein frame due to scale invariance of the dominant R^2 term (in the Jordan frame) during inflation, and predicts the cosmological tilts as well. The basic Starobinsky model can be extended by the subleading (of the higher order in the spacetime curvature) terms leading to the higher powers of $(H_{\text{inf}}^2/m_{\text{S}}^2)$ with the Hubble scale H_{inf} during inflation, which may be needed for a better agreement [16] with more recent CMB observations by Atacama Cosmology Telescope (ACT) [17, 18] and South Pole Telescope (SPT) [19]. The mass scale m_{inf} is determined by the amplitude of primordial scalar perturbations that also fix the energy scale of inflation at $\mathcal{O}(10^{13})$ GeV.

Supersymmetry (SUSY) is the fundamental symmetry relating bosons and fermions, and it is the well-known candidate for new physics beyond the SM, while local SUSY or supergravity automatically implies general relativity. In SUSY, all observed particles have superpartners (sparticles) inside irreducible SUSY multiplets. Since no sparticles were observed so far, SUSY must be spontaneously broken. With conserved R-parity, the lightest sparticle (LSP) is a good candidate for DM.

Supersymmetrising Starobinsky inflation implies a high SUSY scale close to the Starobinsky

inflation scale, thus avoiding no-SUSY constraints from TeV physics and Big Bang Nucleosynthesis (BBN). The success of Starobinsky inflation motivates Starobinsky supergravity as the viable proposal for the gravitational effective action describing high scale inflation. A supergravity realisation of Starobinsky inflation may also determine the structure of the hidden sector together with a specific mechanism of spontaneous SUSY breaking and its mediation to the visible sector. Most of the literature describes that in the Einstein frame, see e.g., Refs. [20–24]. In this paper, we first supersymmetrise the Starobinsky model in the Jordan frame by using the standard (old-minimal) set of supergravity fields [25–31]. Due to the presence of the higher derivatives in the Starobinsky supergravity, the "auxiliary" fields of the old-minimal off-shell supergravity multiplet become physical (propagating) degrees of freedom, which together with other hidden physical degrees of freedom form two chiral supermultiplets called the inflaton supermultiplet \mathcal{T} and the goldstino supermultiplet \mathcal{S} in the Einstein picture. All these hidden degrees of freedom become manifest after a transformation of the Starobinsky supergravity from the Jordan frame to the Einstein frame, and, hence, we consider them as the supergravitational physical degrees of freedom forming the hidden sector where spontaneous SUSY breaking occurs due to the non-vanishing vacuum expectation value (VEV) of \mathcal{S} . As a result, the inflationary dynamics, the hidden sector and SUSY breaking have the single geometrical origin by emerging from the Starobinsky supergravity alone. This approach was pioneered by Hindawi, Ovrut and Waldram in 1995 [32], and further developed by Dalianis, Farakos, Kehagias, Riotto and Unge in 2014 [33].

Connecting inflation to the SM with gravity or to the MSSM with supergravity can be done in several different ways, either in the Einstein frame, see e.g., Refs. [34–40] or in the Jordan frame, see e.g., Refs. [41–43], leading to different results and observable predictions. In this paper, we supersymmetrize Starobinsky inflation in the Jordan frame, but add the MSSM in the Einstein frame, without setting the hidden sector "by hand". This also determines SUSY breaking scale and soft SUSY breaking masses in the MSSM by the energy scale of inflation. The soft masses establish the common high scale SUSY breaking threshold m_0 acting as the upper boundary condition for the renormalisation group (RG) evolution. Below m_0 , the effective low-energy field theory reduces to the SM. The heavy SUSY particles induce threshold corrections to the SM couplings at the matching scale. This procedure also fixes the boundary condition for the Higgs quartic coupling $\lambda(m_0)$. By employing the three-loop RG running, we relate the boundary conditions to the physical observables such as the measured Higgs boson mass. Our results become remarkably predictive and effectively eliminate free parameters typically associated with the phenomenological MSSM, including SUSY breaking scale and gravitino mass.

Another important consequence of our approach concerns the origin of the MSSM μ term. The coupling of the Higgs sector to the hidden sector of Starobinsky supergravity naturally contains the same structural ingredient that is common to singlet-based solutions to the μ problem, where an effective μ parameter is generated when a chiral singlet superfield develops a VEV. However, in contrast to the NMSSM, we do not have to add the singlet "by hand" because it is already present as the goldstino superfield arising from the dual Einstein-frame description of Starobinsky supergravity. Its high scale VEV generates a high scale μ_{eff} of the order of the gravitino mass, provided that the corresponding dimensionless coupling is suppressed. Therefore, our framework realises a high scale supergravitational version of the singlet-generated μ mechanism instead of introducing an independent low energy singlet sector.

In our framework, a viable DM can be obtained with a nearly pure wino as LSP. The observed DM relic abundance selects a physical wino mass close to 2.7–3.0 TeV. This relic density condition determines the target mass of the surviving wino branch. Its realisation in our supergravity framework requires a proper choice of the gauge kinetic function. To realize wino DM, a cancellation between the tree-level gaugino contribution and the anomaly-mediated contribution to the gaugino mass M_2 is required with high precision. The resulting branch is sharply testable both in direct DM detection through the loop-induced spin-independent wino-nucleon cross

section, and at future colliders through the disappearing-track signature of the long-lived charged wino.

The paper is organised as follows. The Starobinsky supergravity setup is introduced in Sec. 2. Inflation and SUSY breaking in the Starobinsky supergravity are considered in Sec. 3. Coupling of the Starobinsky supergravity to the MSSM is described in Sec. 4. Soft MSSM masses and RG running are derived in Sec. 5 that is the key part of this paper. Anomaly mediation of SUSY breaking and wino DM are considered in Sec. 6. Our conclusion is Sec. 7. Estimates of Higgs mass uncertainties and a comparison between SusyHD and HSSUSY codes are given in Appendix A.

2 Starobinsky supergravity setup

A concise and transparent description of $N = 1$ supergravity in four spacetime dimensions is provided by curved superspace [12–14] because of its *manifest* local $N = 1$ supersymmetry, which allows one to construct supergravity actions without a need to check their invariance under SUSY, like in general relativity. We restrict ourselves to the old-minimal supergravity formulation (after the superconformal gauge fixing) that is most suitable for phenomenological applications. We use the standard (Wess-Bagger) notation of Ref. [13] with the reduced Planck mass $M_P = 1$ unless stated otherwise.

We define the Starobinsky supergravity by the following action in curved superspace of the old-minimal supergravity (see Ref. [44] for a review):

$$S_{\mathcal{N}+\mathcal{F}} = \int d^4x d^4\theta E^{-1} \mathcal{N}(\mathcal{R}, \bar{\mathcal{R}}) + \left[\int d^4x d^2\Theta \mathcal{E} \mathcal{F}(\mathcal{R}) + \text{h.c.} \right], \quad (2)$$

in terms of arbitrary non-holomorphic real potential $\mathcal{N}(\mathcal{R}, \bar{\mathcal{R}})$ and holomorphic potential $\mathcal{F}(\mathcal{R})$ depending upon the chiral superfield \mathcal{R} that has the spacetime Ricci scalar R amongst its field components at Θ^2 . The $\bar{\mathcal{R}}$ denotes the anti-chiral superfield obtained by Hermitean conjugation of \mathcal{R} , while E and \mathcal{E} are the supervielbein density and the chiral density in the full and chiral superspace, respectively.

The action (2) is the manifestly supersymmetric extension of the $(R + \alpha R^2)$ gravity because it has only R and R^2 in terms of field components [29]. Equation (2) defines a higher-derivative supergravity (unlike the Einstein supergravity actions in the literature) where the so-called "auxiliary" fields of the old-minimal supergravity, forming the full off-shell supergravity multiplet, become propagating in addition to graviton and gravitino. It is customary in modified gravity or supergravity to refer to such actions as those in the Jordan frame. The chiral $\mathcal{F}(\mathcal{R})$ supergravity [26, 45–47] arises when $\mathcal{N} = 0$.

The spacetime Lagrangian in the action (2) can be rewritten to the chiral form as [31]

$$\mathcal{L} = \int d^2\Theta \mathcal{E} \left[-\frac{1}{8} (\bar{\mathcal{D}}^2 - 8\mathcal{R}) \mathcal{N}(\mathcal{R}, \bar{\mathcal{R}}) + \mathcal{F}(\mathcal{R}) \right] + \text{h.c.}, \quad (3)$$

where the \mathcal{F} -term can be absorbed (up to a constant) into the \mathcal{N} -term. The constant can also be ignored because it leads to a spacetime cosmological constant that we ignore here. Hence, we can use

$$\mathcal{L} = \frac{3}{8} \int d^2\Theta \mathcal{E} (\bar{\mathcal{D}}^2 - 8\mathcal{R}) f(\mathcal{R}, \bar{\mathcal{R}}) + \text{h.c.} \quad (4)$$

that allows us to make a connection to Ref. [33] in terms of the real D -type potential $f(\mathcal{R}, \bar{\mathcal{R}})$ alone.

Though the potential f looks like a Kähler potential in SUSY, this is not the case here because the chiral superfield \mathcal{R} is constrained in superspace supergravity. However, it can be replaced by an unconstrained chiral superfield \mathcal{S} by using a Lagrange multiplier superfield \mathcal{T} as

$$\mathcal{L} = \left[\frac{3}{8} \int d^2\Theta d^2\mathcal{E} (\overline{\mathcal{D}}^2 - 8\mathcal{R}) f(\mathcal{S}, \overline{\mathcal{S}}) + 6 \int d^2\Theta d^2\mathcal{E} \mathcal{T}(\mathcal{S} - \mathcal{R}) \right] + \text{h.c.} \quad (5)$$

On the one hand, varying with respect to \mathcal{T} yields

$$\mathcal{S} = \mathcal{R} \quad (6)$$

that brings back the Lagrangian (4). On the other hand, the last chiral F -type term in the square brackets of (5) can be rewritten to the D -type term in superspace, which leads to

$$\mathcal{L} = \frac{3}{8} \int d^2\Theta d^2\mathcal{E} (\overline{\mathcal{D}}^2 - 8\mathcal{R}) [\mathcal{T} + \overline{\mathcal{T}} + f(\mathcal{S}, \overline{\mathcal{S}})] + \left[6 \int d^2\Theta d^2\mathcal{E} \mathcal{T}\mathcal{S} + \text{h.c.} \right] \quad (7)$$

In its turn, this Lagrangian can be rewritten to the standard form in the Einstein supergravity coupled to chiral matter,

$$\mathcal{L} = \frac{3}{8} \int d^2\Theta d^2\mathcal{E} (\overline{\mathcal{D}}^2 - 8\mathcal{R}) e^{-\frac{1}{3}\mathcal{K}} + \left[\int d^2\Theta d^2\mathcal{E} \mathcal{W} + \text{h.c.} \right], \quad (8)$$

with the Kähler potential \mathcal{K} and superpotential \mathcal{W} given by

$$\mathcal{K} = -3 \ln[\mathcal{T} + \overline{\mathcal{T}} + f(\mathcal{S}, \overline{\mathcal{S}})], \quad \mathcal{W} = 6\mathcal{T}\mathcal{S}, \quad (9)$$

for two chiral matter superfields \mathcal{S} and \mathcal{T} .¹ The field theory (8) does not have the higher derivatives and defines the equivalent (or dual) Lagrangian in the Einstein frame. Because of their supergravitational origin, the matter superfields \mathcal{S} and \mathcal{T} form the hidden sector in the Einstein supergravity in addition to other matter like the MSSM that can be added to the supergravity action (8). The dependence of the Kähler potential (9) upon \mathcal{T} has the "no-scale" form that establishes a connection to the no-scale supergravity models [20–24].

The Starobinsky supergravity defines the supergravity framework in the Jordan frame, like $F(R)$ gravity defines the framework for the Starobinsky model of inflation, see e.g., Ref. [48] for the latter. Describing viable Starobinsky inflation in the Starobinsky supergravity requires carefully chosen potentials $f(\mathcal{R}, \overline{\mathcal{R}})$. Unlike the modified $F(R)$ gravity that has only one (hidden) scalar physical degree of freedom, the Starobinsky supergravity has four scalar physical degrees of freedom associated with the leading (complex) field components of two chiral matter superfields. In general, this leads to multi-field inflation in supergravity [49] where all scalars contribute to the scalar potential and can easily destabilise inflation leading to a very few e-folds and large iso-curvature perturbations. Therefore, one has to stabilise three scalars out of four of them in order to get effectively single-field inflation driven by the remaining scalar called inflaton, see e.g., Ref. [31] for details and the way to embed and stabilise the single-field Starobinsky inflation in the Starobinsky supergravity. In addition, since inflation implies positive energy, a supergravity realisation of inflation is always accompanied by spontaneous SUSY breaking that, in turn, implies the existence of a physical Nambu-Goldstone spin-1/2 fermion called goldstino. In the Starobinsky supergravity, inflaton belongs to the chiral superfield \mathcal{T} , whereas goldstino belongs to the chiral superfield \mathcal{S} . In the supergravity realisations of inflation, the goldstino superfield \mathcal{S} is usually stabilised at its origin by assigning its heavy mass beyond the Hubble value during inflation.

Going from the superfield formulation of a supergravity theory to its formulation in terms of the field components of the supergravity superfields is a tedious procedure requiring (i) fixing

¹After rescaling the dimensionless superfields \mathcal{T} and \mathcal{S} to the canonical dimension (one), the coupling constant appears in front of the superpotential \mathcal{W} .

the gauge invariance against superdiffeomorphisms in curved superspace, (ii) removing auxiliary fields, and (iii) rescaling or redefining the remaining fields to get canonical normalisations of their kinetic terms [12–14]. Fortunately, in the Einstein frame, one only needs to know a Kähler potential K and a superpotential W or, actually, their Kähler-gauge-invariant combination $G = K + \ln(W\bar{W})$.

The physical field content of the Starobinsky supergravity (in the Einstein frame, without adding matter, and after eliminating the auxiliary fields) is given by

- graviton e_μ^a or $g_{\mu\nu}$ and gravitino ψ_μ^a of spin 2, where both flat (a) and curved (μ) indices take four values,
- real inflaton $\text{Re}(T)$, axion (or sinflaton) $\text{Im}(T)$ of spin 0, and inflatino fermion χ_T of spin 1/2,
- complex sgoldstino S of spin 0 and goldstino fermion χ_S of spin 1/2.

These fields are subject to the residual gauge transformations, including local SUSY leading to equal total numbers of the bosonic and fermionic (on-shell) degrees of freedom. However, these SUSY transformations are now dependent upon the supergravity theory chosen, while their algebra is closed only on the equations of motion.

Starobinsky inflation ending in a Minkowski vacuum can be realised by using the function [33]

$$f(\mathcal{R}, \bar{\mathcal{R}}) = 1 - 2\frac{\mathcal{R}\bar{\mathcal{R}}}{m^2} + \frac{1}{9}\zeta\frac{\mathcal{R}^2\bar{\mathcal{R}}^2}{m^4}, \quad (10)$$

where, on the right-hand-side, the first term generates the Einstein supergravity as the SUSY extension of the Einstein-Hilbert Lagrangian, the second term generates the R^2 -supergravity, whereas the last term with the dimensionless coupling constant ζ is needed to stabilise the additional scalar degrees of freedom (beyond inflaton) during inflation; without the quartic term, the inflationary trajectory suffers from a tachyonic instability [31]. The mass parameter m in eq. (10) is essentially the Starobinsky mass of the order 10^{13} GeV.

The Starobinsky supergravity defined by Eq. (10) has exact R-symmetry, and its vacuum structure is controlled by the stabilization parameter ζ . To support a single-field inflation, this parameter must satisfy the stability bound $\zeta > 3.54$ but then inflaton ends up in a SUSY-preserving vacuum [32]. A Minkowski vacuum with broken SUSY is only possible with $\zeta = 1$ but this value is incompatible with stable inflation for enough numbers of e-folds. Hence, in order to get a spontaneously broken SUSY after inflation in a Minkowski vacuum, one has to add R-symmetry breaking terms to the f -function, though without destroying Starobinsky inflation and without generating a cosmological constant. The minimal realisation of this task amounts to adding linear terms to the f -function (10) as follows [33]:

$$f(\mathcal{R}, \bar{\mathcal{R}}) = 1 + \gamma\frac{\mathcal{R} + \bar{\mathcal{R}}}{m} - 2\frac{\mathcal{R}\bar{\mathcal{R}}}{m^2} + \frac{1}{9}\zeta\frac{\mathcal{R}^2\bar{\mathcal{R}}^2}{m^4} \quad (11)$$

with the new coupling constant γ as the source of explicit R-symmetry breaking. This adjustment eliminates the constraints found in the R-symmetric case, enables the existence of a Minkowski vacuum with broken SUSY and no massless R-axion, while simultaneously supporting a viable single-field inflationary phase driven by the R^2 term like that in the Starobinsky model. In addition, this leads to heavy scalar particles in the hidden sector.

3 Scalar potential, inflation and gravitino mass

The scalar sector of the Lagrangian (8) has the form

$$e^{-1}\mathcal{L} = -\frac{1}{2}R - \mathcal{K}_{i\bar{j}}\partial z^i\partial\bar{z}^{\bar{j}} - \mathcal{V}(z^i, \bar{z}^{\bar{i}}), \quad (12)$$

where $\mathcal{K}_{i\bar{j}}$ is the Kähler metric derived from the Kähler potential \mathcal{K} , and \mathcal{V} is the scalar potential of the complex scalar fields z^i collectively representing the leading scalar field components T and S of the chiral superfields \mathcal{T} and \mathcal{S} . The scalar potential is given by the standard formula [13]

$$\mathcal{V} = e^{\mathcal{K}} \left[(\mathcal{K}^{-1})^{i\bar{j}} (\mathcal{D}_i\mathcal{W})(\mathcal{D}_{\bar{j}}\bar{\mathcal{W}}) - 3\mathcal{W}\bar{\mathcal{W}} \right], \quad (13)$$

where $\mathcal{D}_i\mathcal{W} = \partial_i\mathcal{W} + (\partial_i\mathcal{K})\mathcal{W}$ is the Kähler covariant derivative.

The choice (11) for the master function $f(\mathcal{R}, \bar{\mathcal{R}})$ from the preceding Sect. 2 leads to the following Kähler potential and superpotential:

$$\mathcal{K} = -3M_{\text{P}}^2 \ln \left\{ 1 + \frac{\mathcal{T} + \bar{\mathcal{T}}}{M_{\text{P}}} + \gamma \frac{\mathcal{S} + \bar{\mathcal{S}}}{M_{\text{P}}} - 2 \frac{\mathcal{S}\bar{\mathcal{S}}}{M_{\text{P}}^2} + \frac{1}{9}\zeta \frac{\mathcal{S}^2\bar{\mathcal{S}}^2}{M_{\text{P}}^4} \right\}, \quad \mathcal{W} = 6m\mathcal{T}\mathcal{S}, \quad (14)$$

where we have reintroduced the reduced Planck mass M_{P} for more transparency from the physical viewpoint.

When parametrising the scalar fields as $T/M_{\text{P}} = t + ib$ and $S/M_{\text{P}} = s + ic$, one can demonstrate that the imaginary field components are stabilised at the origin with $\langle b \rangle = \langle c \rangle = 0$. Consequently, the scalar potential is reduced to a function of the real field components t and s . We find (see also Ref. [33])

$$\mathcal{V}(t, s) = 12m^2M_{\text{P}}^2 \frac{s^2 \left\{ 1 - 2s^2 + \zeta s^4 - 2\gamma s \right\} + \frac{9}{2} \frac{[t - \gamma s - \frac{2}{3}s^2(3 - \zeta s^2)]^2}{(9 - 2\zeta s^2)}}{(1 - 2s^2 + \zeta s^4 + 2t + 2\gamma s)^2}. \quad (15)$$

Demanding this potential to have a local minimum corresponding to a Minkowski vacuum with $\langle \mathcal{V} \rangle = 0$ and spontaneously broken SUSY with $\langle \mathcal{D}_i\mathcal{W} \rangle \neq 0$ constrains the parameters ζ and γ . Specifically, these conditions imply [33]

$$\zeta = \frac{1 + 2s_0^2}{3s_0^4} \quad \text{and} \quad \gamma = -2s_0 + \frac{2 + 4s_0^2}{3s_0}, \quad (16)$$

where $s_0 = \langle s \rangle$, thus leaving only two independent parameters, namely, the VEV s_0 and the mass scale m .

The gravitino mass evaluated at the post-inflation minimum is determined by another standard formula in supergravity [13],

$$m_{3/2}^2 = \langle e^G \rangle = \langle e^{\mathcal{K}} |\mathcal{W}|^2 \rangle = \frac{24m^2s_0^2(1 + 2s_0^2)^2}{11 - 14s_0^2}, \quad (17)$$

where we have used Eqs. (14), (15) and (16) in the last equation. To get a positive gravitino mass squared, the VEV of the s -field must obey the condition [33]

$$|s_0| < \sqrt{\frac{11}{14}} \quad (18)$$

that restricts a position of the vacuum. Furthermore, this also imposes the constraints on the parameters governing the potential, namely,

$$\gamma > 0.16 \quad \text{and} \quad \zeta > 1.38. \quad (19)$$

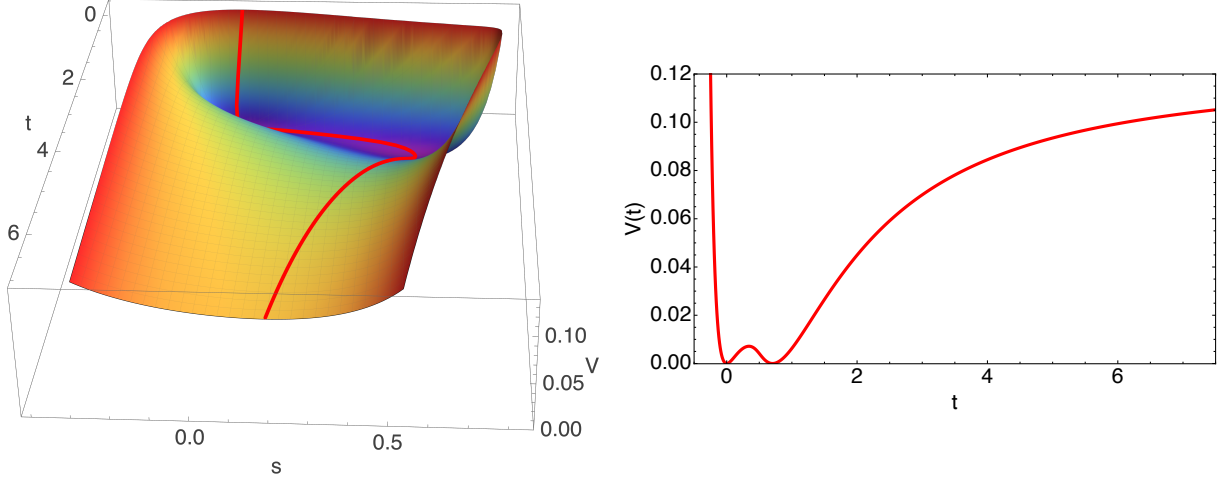


Figure 1: The scalar potential $\mathcal{V}(t, s)$ overlaid by the $\partial\mathcal{V}/\partial s = 0$ trajectory is on the left-hand side. Due to its large effective mass, the field s is stabilised at the minimum of the potential for any given t , leading to a function $s = \mathcal{Q}(t)$. A slice of the scalar potential along the $\partial\mathcal{V}/\partial s = 0$ trajectory is on the right-hand side.

During inflation, the scalar field s slowly oscillates near a local minimum of the potential for any given value of the inflaton t . The minimum is determined by the condition $\partial\mathcal{V}(t, s)/\partial s = 0$ that leads to $s = \mathcal{Q}(t)$ and the effective potential $\mathcal{V}(t) \equiv \mathcal{V}(t, \mathcal{Q}(t))$ leading to single-field dynamics governed by the Lagrangian

$$e^{-1}\mathcal{L}_{\text{eff}} = -\frac{M_{\text{P}}^2}{2}R - \frac{1}{2}K(t)\partial_\mu t\partial^\mu t - \mathcal{V}(t) \quad (20)$$

Given the non-canonical kinetic term, the inflationary dynamics is described by the generalized slow-roll parameters defined by

$$\epsilon_K(t) = \frac{1}{2}M_{\text{P}}^2 \frac{(\mathcal{V}'(t))^2}{K(t)\mathcal{V}(t)^2} \quad \text{and} \quad \eta_K(t) = M_{\text{P}}^2 \frac{\mathcal{V}''(t)}{K(t)\mathcal{V}(t)} - \frac{1}{2}M_{\text{P}}^2 \frac{K'(t)\mathcal{V}'(t)}{K(t)^2\mathcal{V}(t)}. \quad (21)$$

The duration of inflation in terms of e-folds N from a field value t to the end of inflation t_e defined by $\epsilon_K(t_e) = 1$ is given by

$$N(t) = \int_{t_e}^t \frac{K(\tilde{t})\mathcal{V}(\tilde{t})}{M_{\text{P}}^2\mathcal{V}'(\tilde{t})} d\tilde{t}. \quad (22)$$

The scalar amplitude A_s , the scalar spectral index n_s , and the tensor-to-scalar ratio r are evaluated at the horizon crossing on the pivot scale denoted by N as

$$A_s = \frac{\mathcal{V}(t(N))}{24\pi^2 M_{\text{P}}^4 \epsilon_K(t(N))} \approx 2.1 \cdot 10^{-9} \quad (23)$$

and

$$n_s = 1 - 6\epsilon_K(t(N)) + 2\eta_K(t(N)), \quad r = 16\epsilon_K(t(N)). \quad (24)$$

To extract the physical mass in the presence of a non-canonical kinetic term for a scalar ϕ , one should make a field redefinition to a canonical scalar field $\hat{\phi}$. In general, given a field ϕ with a kinetic function $\mathcal{B}(\phi)$, the transform yields the canonical mass squared $m_{\hat{\phi}}^2 = \frac{\langle \mathcal{V}''(\phi) \rangle}{\langle \mathcal{B} \rangle}$ to be evaluated at the potential minimum. This way we get the canonical squared masses m_c^2/H^2 , m_y^2/H^2 and m_b^2/H^2 with $y = s - \mathcal{Q}(t)$, while the potential has a minimum at $y = 0$. The results are given in Fig. 2 (a)-(c). All those canonical masses are above the Hubble scale H_{inf} during

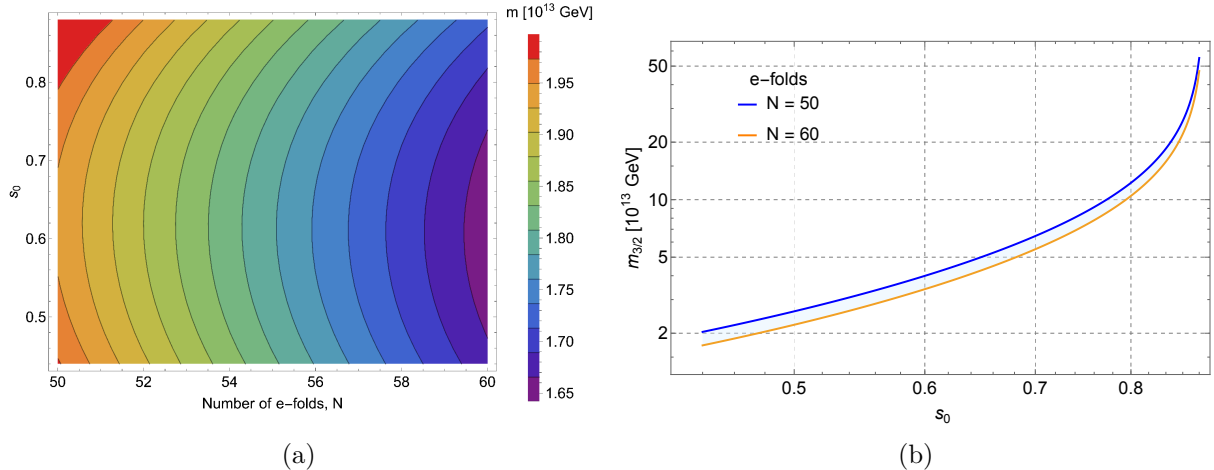


Figure 2: **(a)** Numerical evaluation of the inflaton mass parameter m (in units of 10^{13} GeV) as a function of the pivot e-folds N over the interval $[50, 60]$ and the goldstino VEV s_0 in the allowed interval $(0.438, 0.886)$. **(b)** Gravitino mass $m_{3/2}$ (in units of 10^{13} GeV) as a function of the goldstino VEV s_0 in the log log scale. The thin band in light blue highlights the variation of the results across the range of e-folds in the interval $[50, 60]$.

inflation for all relevant values of s_0 . This confirms that the fields b , c and y are effectively frozen during inflation driven by the inflaton t .

The results of our numerical calculations for the e-folds N belonging to the interval $[50, 60]$ against the Planck 2018 and ACT DR6 confidence contours, and against the Starobinsky model predictions are given in Fig. 3(d), being in excellent agreement with observations. The predicted values of n_s slightly increase in our supergravity model against those in the original Starobinsky model toward better agreement with ACT observations at 2σ confidence level. Equation (23) determines the mass parameter m from the observed CMB amplitude A_s and the number of e-folds N .

The mass m depends not only upon N but slightly upon the goldstino VEV s_0 also. A numerical evaluation of m over the intervals $[50, 60]$ for N and $(0.438, 0.886)$ for s_0 shows that m should belong to the interval $(1.65, 1.98) \times 10^{13}$ GeV. This value of m is lower than the standard Starobinsky mass given by

$$m_S = \sqrt{24\pi^2 A_s} \left(\frac{M_P}{N} \right) = 3.4 \left(\frac{50}{N} \right) \cdot 10^{13} \text{ GeV} . \quad (25)$$

The value of m in our framework links the cosmological evolution to the scale of SUSY breaking in the hidden sector, where the goldstino VEV s_0 determines the gravitino mass $m_{3/2}$ according to Eq. (17).

The theoretical and phenomenological consistency of our model imposes strict bounds on the goldstino VEV s_0 . To ensure a positive gravitino mass squared and vacuum stability, s_0 must satisfy Eq. (18), i.e. $|s_0| < \sqrt{11/14} \approx 0.886$. In order to prevent a catastrophic gravitino overproduction, the decay channel of inflaton into two gravitino should be forbidden, which implies the kinematic condition $m_{inf} < 2m_{3/2}$, where m_{inf} is the canonically normalized mass of the inflaton field t in vacuum. The kinematic threshold corresponds to $s_0 \approx 0.438$ and is indicated by the orange dotted line in Fig. 3, thereby restricting the viable parameter space of s_0 to $(0.438, 0.886)$.

Possible small variations in the predictions for the cosmological tilts (n_s, r) may also be explained within Starobinsky supergravity by adding higher powers of \mathcal{R} and $\bar{\mathcal{R}}$, or an additional dependence upon other superfields of the superspace supergravity (perhaps involving their covariant

derivatives), to the master function f in Eq. (4); see, e.g., Refs. [16, 26, 50]. Yet another possible option could be non-instantaneous reheating, which increases the value of N [51].

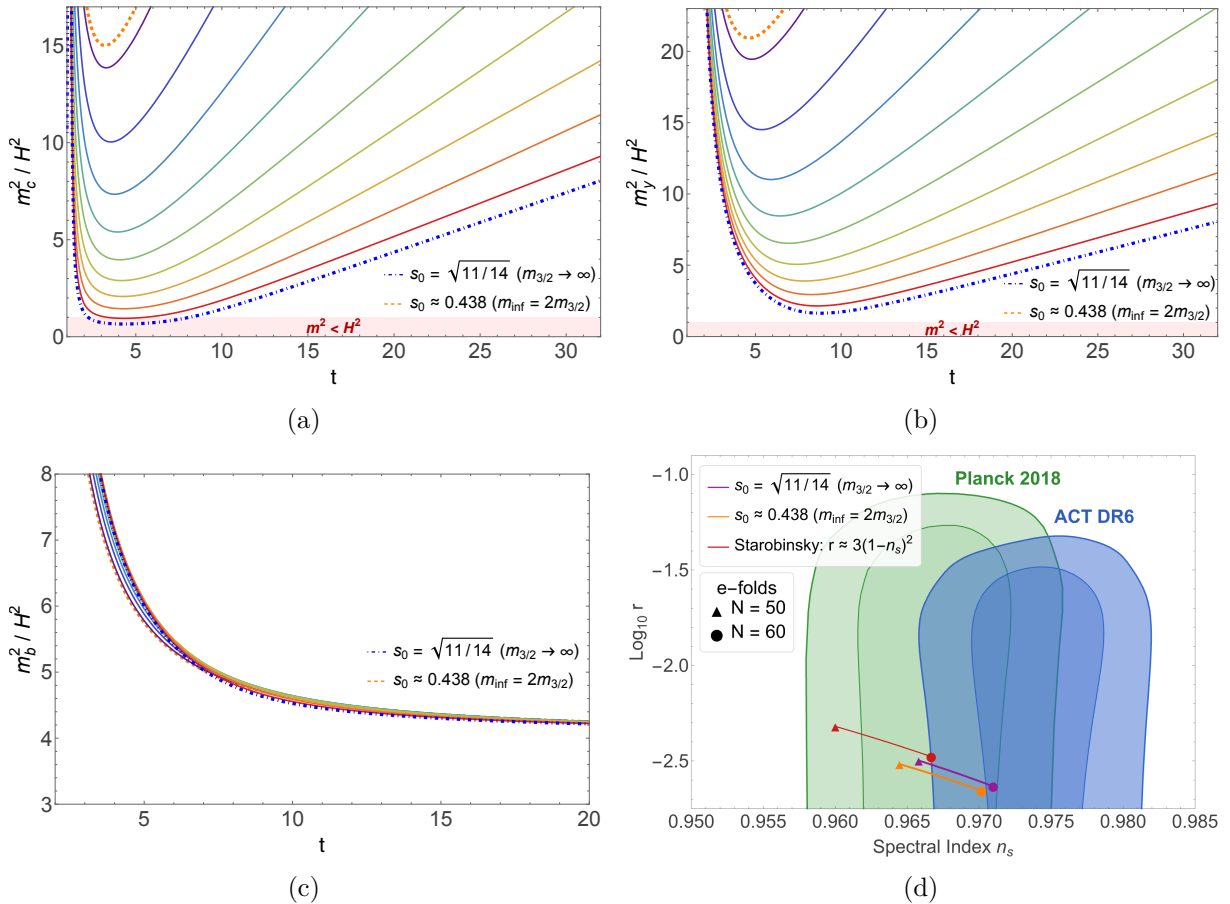


Figure 3: The evolution of the scalar masses in the hidden sector and the cosmological predictions. **(a)–(c)**: The effective squared masses m_c^2/H^2 , m_y^2/H^2 and m_b^2/H^2 as the functions of the inflaton field t during inflation. The blue line represents the stability bound $s_0 = \sqrt{11/14}$ ($m_{3/2} \rightarrow \infty$), and the red line corresponds to the kinematic decay threshold $s_0 \approx 0.438$ ($m_{\text{inf}} = 2m_{3/2}$). The light red shaded region at the bottom marks the boundary $m^2 < H^2$. **(d)**: Our predictions for the spectral index n_s and the tensor-to-scalar ratio $\log_{10} r$ evaluated for e-folds N in the interval [50, 60], compared against the 1σ and 2σ confidence contours from the Planck 2018 [52] and ACT DR6 data [17, 18].

As is clear from Fig. 3 (d), our predictions for n_s and r are in good agreement with observations. For details on the differences between the Planck and ACT constraints, see Refs. [53, 54].

4 Coupling of Starobinsky supergravity to MSSM

There are several different ways to couple the MSSM to the Starobinsky supergravity, either in the Jordan frame or in the Einstein frame, either in terms of superfields or in terms of fields. For instance, when the superfield MSSM is coupled to the Starobinsky supergravity in the Jordan frame, this leads to the Kähler potential

$$\mathcal{K} = -3M_{\text{P}}^2 \ln \left(1 + \frac{\mathcal{T} + \bar{\mathcal{T}}}{M_{\text{P}}} + \gamma \frac{\mathcal{S} + \bar{\mathcal{S}}}{M_{\text{P}}} - 2 \frac{\mathcal{S}\bar{\mathcal{S}}}{M_{\text{P}}^2} + \frac{1}{9} \zeta \frac{\mathcal{S}^2 \bar{\mathcal{S}}^2}{M_{\text{P}}^4} + \sum_A \frac{\bar{\Phi}_A \Phi_A}{M_{\text{P}}^2} \right) \quad (26)$$

with non-canonical kinetic terms for all MSSM chiral superfields Φ_A .

Another option is choosing the manifestly supersymmetric coupling of the MSSM matter in the *Einstein* frame, in order to have the *canonical* kinetic terms for the MSSM matter with a “renormalizable” superpotential up to the 3rd order in the chiral superfields Φ_A . Then the Kähler potential and the superpotential are given by

$$\mathcal{K} = -3M_{\text{P}}^2 \ln \left(1 + \frac{\mathcal{T} + \bar{\mathcal{T}}}{M_{\text{P}}} + \gamma \frac{\mathcal{S} + \bar{\mathcal{S}}}{M_{\text{P}}} - 2 \frac{\mathcal{S}\bar{\mathcal{S}}}{M_{\text{P}}^2} + \frac{1}{9} \zeta \frac{\mathcal{S}^2 \bar{\mathcal{S}}^2}{M_{\text{P}}^4} \right) + \sum_A \bar{\Phi}_A \Phi_A, \quad (27)$$

and

$$\mathcal{W} = 6m\mathcal{T}\mathcal{S} + \mathcal{W}_{\text{MSSM}}(\Phi_A), \quad (28)$$

where

$$\mathcal{W}_{\text{MSSM}}(\Phi_A) = \mu H_u H_d + \sum_{A,B,C} y_{ABC} \Phi_A \Phi_B \Phi_C, \quad (29)$$

and the sums go over the MSSM chiral matter superfields

$$\Phi_A = (Q, L, d^c, u^c, e^c, H_d, H_u). \quad (30)$$

The first term in Eq. (29) is called the μ -term, and y_{ABC} are the MSSM Yukawa coupling constants.² In what follows, μ should be understood either as an effective parameter in the MSSM superpotential at the matching scale or as a quantity dynamically generated by the hidden sector, as discussed below. The chiral matter sector in the MSSM is coupled to the gauge matter sector described by vector gauge superfields, see e.g., Ref. [58] for details.

SUSY breaking in the hidden sector can be mediated to the MSSM sector at the tree level via gravitational couplings in the field Lagrangian derived from the \mathcal{K} and the \mathcal{W} . In turn, this generates soft SUSY breaking terms in the MSSM after decoupling of gravity at smaller scales. Equations (26) and (27) lead to different soft terms and different physics. In what follows, we proceed with Eq. (27).

The μ -term in Eq. (29) can be dynamically generated from interactions between the Higgs sector and the hidden sector of supergravity. This mechanism is structurally the same as singlet-based solutions of the μ -problem, such as the Next-to-Minimal Supersymmetric Standard Model (NMSSM), where an effective supersymmetric Higgs mass is generated when a gauge-singlet chiral superfield develops a VEV, $\mu_{\text{eff}} = \lambda \langle N \rangle$ [59, 60]. The important difference is that in the present construction the singlet is not added as an extra low-energy sector. The required chiral superfield is already present as the goldstino multiplet \mathcal{S} emerging from Starobinsky supergravity in the Einstein frame.

For instance, the μ -term of the order of the gravitino mass, $\mu \sim \mathcal{O}(m_{3/2})$, can arise from the Kähler potential via the standard Giudice-Masiero mechanism [61, 62]. Alternatively, in our framework the μ -term can be generated from the superpotential interaction

$$\frac{\tilde{\lambda}}{M_{\text{P}}^{n-1}} \mathcal{S}^n H_u H_d, \quad (31)$$

where $\tilde{\lambda}$ is a dimensionless coupling. Since the scalar component of the goldstino superfield \mathcal{S} acquires the Planck-scale VEV $\langle \mathcal{S} \rangle = s_0 M_{\text{P}}$ after inflation, this interaction generates

$$\mu = \tilde{\lambda} s_0^n M_{\text{P}}. \quad (32)$$

Thus the model contains the same basic ingredient as singlet-generated μ -mechanisms, but embeds it into the supergravitational hidden sector rather than into an extra low-energy singlet

²Indices for three particle generations are suppressed. The non-vanishing Yukawa couplings are for (Q, H_d, d^c) , (Q, H_u, u^c) and (L, H_d, e^c) . The Yukawa couplings are not derivable in supergravity but may be selected from string theory compactification [55–57].

sector. Since $\langle S \rangle$ is of order M_{P} , obtaining $\mu \sim m_{3/2} \sim 10^{13}$ GeV requires a suppressed dimensionless coupling $\tilde{\lambda} \sim m_{3/2}/M_{\text{P}}$, up to powers of the dimensionless s_0 . Such a suppression can be dynamically realised if $\tilde{\lambda}$ is generated by non-perturbative effects, for example, by instantons [55–57]. The phenomenologically viable value of n is fixed below by the Higgs sector boundary conditions. See Ref. [63] for a review of the μ -problem and its possible solutions.

A direct phenomenological consequence is that the higgsinos are heavy in the high-scale solutions considered here. Since μ_{eff} is tied to the gravitino mass scale, the higgsino states decouple together with the scalar superpartners and cannot provide a TeV-scale higgsino LSP.

5 Soft MSSM parameters and RG running

Having obtained the Kähler potential \mathcal{K} and the superpotential \mathcal{W} as sums of contributions from the hidden and MSSM sectors, one can derive soft SUSY breaking terms. To obtain the low-energy effective Lagrangian, we apply the standard procedure of taking the “flat limit” [64, 65] by sending $M_{\text{P}} \rightarrow \infty$ while keeping $m_{3/2}$ fixed. In this limit, all soft scalar masses, trilinear and bilinear couplings are derived from an expansion of the scalar potential in supergravity. When the auxiliary fields F^m of the hidden sector superfields acquire non-zero VEVs, the effective mass terms for squarks, sleptons and Higgs bosons, as well as the trilinear A -terms and bilinear B -terms, are generated. The gaugino masses are generated from gaugino couplings to the F -terms via a holomorphic gauge kinetic function f_a . Communication of SUSY breaking from the hidden sector to the MSSM sector is therefore mediated by gravity at the classical level, with additional anomaly-mediated contributions generated at the quantum level.

The general setup of Refs. [64, 65] in terms of physical fields of the MSSM matter superfields is greatly simplified in our case with the Kähler potential in Eq. (27) and the superpotential in Eq. (28). In particular, the soft scalar masses are given by

$$m_{\tilde{\alpha}\tilde{\beta}}^2 = m_{3/2}^2 \delta_{\tilde{\alpha}\tilde{\beta}} \quad \text{or} \quad m_0 = m_{3/2} . \quad (33)$$

The universal trilinear parameter A is given by a contraction of the hidden sector F-terms with the derivatives of the Kähler potential, $A = F^m \partial_m \mathcal{K}$. With the Kähler potential in Eq. (27), we find

$$A = m_{3/2} \left[3 - \frac{2(11 - 5s_0^2)}{3(1 + 2s_0^2)} \right] = m_{3/2} \frac{28s_0^2 - 13}{3(1 + 2s_0^2)} . \quad (34)$$

In the absence of bilinear mixing terms in the Kähler potential, the bilinear soft parameter B reduces to $B = F^m \partial_m \mathcal{K} - m_{3/2}$ and reads

$$B = A - m_{3/2} = m_{3/2} \frac{2(11s_0^2 - 8)}{3(1 + 2s_0^2)} . \quad (35)$$

The physical Higgs mixing parameter μ_{eff} is derived from the superpotential coupling constant μ after rescaling as

$$\mu_{\text{eff}} = e^{\langle \mathcal{K} \rangle / 2} \mu . \quad (36)$$

The gaugino masses M_a are determined by the diagonal elements of the gauge kinetic function f_a as [64, 65]

$$M_a = \frac{1}{2} (\text{Re} f_a)^{-1} F^m \partial_m f_a . \quad (37)$$

When adopting a linear *Ansatz*, $f_a = (1 + c_T T + c_S S)$ with the parameters c_T and c_S , on the tree level we get

$$M_a = m_{3/2} \frac{2(11 - 5s_0^2) [2c_T(1 + 2s_0^2) + 9c_S s_0]}{9(1 + 2s_0^2) [9 + 4c_T(1 + 2s_0^2) + 9c_S s_0]} = m_{1/2} . \quad (38)$$

Therefore, as may have been expected, the entire MSSM soft spectrum on the high scale is proportional to the gravitino mass $m_{3/2}$. The VEV s_0 is dynamically generated by the fundamental R-symmetry breaking parameter γ , while the gravitino mass $m_{3/2}$ is tied to the Starobinsky inflation scale $m \sim 10^{-5} M_P$ via the vacuum relation (17).

To connect the high-scale SUSY predictions to the EW-scale observables, we use two independent effective field theory (EFT) implementations, `SusyHD` [66] and `HSSUSY` within `FlexibleSUSY` [67–69]. Both codes match the MSSM onto the SM at the high SUSY scale and re-sum the large logarithms generated by the wide separation between the EW and SUSY breaking scales through RG evolution. We use `SusyHD` for the main parameter scans and `HSSUSY` as an independent cross-check of selected benchmark points and uncertainty estimates. This comparison tests the stability of the Higgs mass prediction against differences in the implementation of threshold corrections, the extraction of the low-energy SM parameters, and the treatment of the renormalisation scales. The soft spectrum above serves as the initial condition for RG running. When following the standard high-scale SUSY scenario [70], the MSSM is directly mapped onto the SM at the scale $m_0 = m_{3/2}$. Below the matching scale, the heavy sparticles are integrated out. The boundary condition for the SM Higgs quartic coupling $\lambda(m_0)$ is determined by the MSSM tree-level relation combined with the high-scale threshold corrections $\Delta\lambda$ as

$$\lambda(m_0) = \frac{1}{4} \left[g_2^2(m_0) + \frac{3}{5} g_1^2(m_0) \right] \cos^2 2\beta + \Delta\lambda . \quad (39)$$

The threshold corrections are sensitive to the stop-mixing parameter $X_t = A_t - \mu_{\text{eff}} \cot \beta$ and include the full one-loop contributions and the leading two-loop supersymmetric contributions. The stop-mixing parameter X_t must be constrained in order to prevent the formation of colour- and charge-breaking (CCB) minima along the squark field directions [70]. More specifically, demanding that a CCB minimum is not deeper than the standard EW minimum dictates an upper bound on the stop mixing. Since all supersymmetric scalars in our framework acquire the universal high-scale mass $m_{3/2}$, the stability condition takes the form

$$\frac{(A_t - \mu_{\text{eff}} \cot \beta)^2}{m_{3/2}^2} < 8 - \frac{2}{\sin^2 \beta} . \quad (40)$$

The Higgs coupling λ is evolved down to the EW scale according to the three-loop RG equations. This procedure effectively resums large logarithms of the form $\ln(m_{3/2}/m_t)$. The physical Higgs boson pole mass M_h is determined at the top mass scale by the relation

$$M_h^2 = v^2 [\lambda(m_t) + \delta\lambda(m_t)] , \quad (41)$$

where $v \simeq 246.22$ GeV is the Higgs VEV. The term $\delta\lambda(m_t)$ represents the finite threshold corrections computed up to two loops, which are required for matching the running parameters with the physical mass. The SM Higgs doublet is given by a linear combination of the two MSSM Higgs doublets H_u and H_d as

$$H_{\text{SM}} = H_u \sin \beta + H_d^\dagger \cos \beta \quad (42)$$

with the mixing angle β .

In our framework, both Higgs doublets acquire the large soft masses $m_{H_u} = m_{H_d} = m_{3/2}$. For a light SM Higgs doublet to exist well below the SUSY breaking scale, the tree-level Higgs mass-squared matrix should have one eigenvalue much smaller than the characteristic SUSY scale, $m_{\text{light}}^2 \ll m_{3/2}^2$, whereas the other eigenvalue stays heavy, $m_{\text{heavy}}^2 \sim m_{3/2}^2$. The determinant of the Higgs sector mass-squared matrix can be expressed in terms of these eigenvalues as follows:

$$\det(\mathcal{M}_H^2) = (m_{H_u}^2 + \mu_{\text{eff}}^2)(m_{H_d}^2 + \mu_{\text{eff}}^2) - (B\mu_{\text{eff}})^2 = m_{\text{light}}^2 m_{\text{heavy}}^2 . \quad (43)$$

Thus, the existence of a light SM-like Higgs doublet requires a cancellation between the diagonal and off-diagonal contributions to \mathcal{M}_H^2 , so that $\det(\mathcal{M}_H^2) \ll m_{3/2}^4$. This is the usual EW fine-tuning in high-scale SUSY. At leading order, the cancellation can be formulated as the high-scale boundary condition

$$\det(\mathcal{M}_H^2) = 0 \quad (44)$$

with high precision. As shown below, in our framework this leads to an equation on the goldstino VEV s_0 . After substituting the universal soft scalar masses $m_{H_u} = m_{H_d} = m_{3/2}$ into Eq. (44), we get

$$m_{3/2}^2 + \mu_{\text{eff}}^2 = |B\mu_{\text{eff}}| . \quad (45)$$

By dividing both sides by $m_{3/2} |\mu_{\text{eff}}|$, this relation can be rewritten in terms of the dimensionless ratio $x \equiv |\mu_{\text{eff}}|/m_{3/2} > 0$ as

$$x + \frac{1}{x} = \frac{|B|}{m_{3/2}} . \quad (46)$$

Since $x + 1/x \geq 2$ for any $x > 0$, this imposes a lower bound on the bilinear soft parameter,

$$|B| \geq 2m_{3/2} . \quad (47)$$

Inserting Eq. (45) into the minimization condition for the Higgs potential,

$$\sin 2\beta = \frac{2B\mu_{\text{eff}}}{m_{H_u}^2 + m_{H_d}^2 + 2\mu_{\text{eff}}^2} , \quad (48)$$

implies $|\sin 2\beta| = 1$ or, equivalently, $|\tan \beta| = 1$ up to small corrections of the order $\mathcal{O}(m_{\text{light}}/m_{3/2})$. Therefore, as implied by Eq. (39) and Eq. (41), the physical Higgs boson mass is almost entirely generated by radiative threshold corrections and the subsequent RG running.

Regarding the high-scale boundary condition for the stop-mixing parameter $X_t = A_t - \mu_{\text{eff}} \cot \beta$, we adopt the minimal choice $X_t = 0$. This condition is imposed to suppress the high-scale threshold corrections to the Higgs quartic coupling. Assuming $X_t = 0$ also ensures the stability of the vacuum along the squark directions and avoids CCB minima [70]. Given the universality ($A_t = A$), this assumption yields $\mu_{\text{eff}} = A \tan \beta$. Inserting this relation back into Eq. (48), we can safely remove the absolute value in Eq. (45), yielding $BA > 0$ and $\tan \beta = 1$.

Finally, given $\tan \beta = 1$, the condition $X_t = 0$ dictates $A = \mu_{\text{eff}}$. Equations (35) and (45) then imply

$$m_{3/2}^2 + A^2 = A(A - m_{3/2}) \quad \text{and, hence,} \quad A = -m_{3/2} , \quad (49)$$

which fixes the parameter $\mu_{\text{eff}} = -m_{3/2}$. Then taking into account Eq. (36) allows us to express the parameter μ in Eq. (29) in terms of the mass scale m and the VEV of \mathcal{S} as

$$\mu = -\frac{8}{3}ms_0(1 + 2s_0^2) . \quad (50)$$

The relation $A = -m_{3/2}$ together with Eq. (35) lead to a consistency condition on s_0 ,

$$\frac{28s_0^2 - 13}{3(1 + 2s_0^2)} = -1 \quad \text{or} \quad s_0 = \sqrt{\frac{5}{17}} \approx 0.542 \quad \text{and} \quad \gamma = \frac{8}{\sqrt{85}} \approx 0.868 . \quad (51)$$

Having fixed the VEV $s_0 = \sqrt{5/17}$, we are able to calculate the mass scale m and, consequently, the gravitino mass $m_{3/2}$. The numerical analysis of the inflationary dynamics in the preceding Section related the mass scale m to the known amplitude A_s of CMB scalar perturbations. For example, when assuming the middle value of e-folds $N_* = 55$ with the pivot scale $k = 0.05 \text{ Mpc}^{-1}$

crossing the horizon, we find $m \approx 1.78 \times 10^{13}$ GeV. After substituting this value of m into the vacuum relation (17) defining the gravitino mass, we obtain the middle value

$$m_{3/2} \approx 2.86 \times 10^{13} \text{ GeV} . \quad (52)$$

Summarising the above, this Section leads to the following high-energy boundary conditions for RG running:

$$\tan \beta = 1, \quad m_0 = m_{3/2}, \quad A = \mu_{\text{eff}} = -m_{3/2}, \quad B = -2m_{3/2}. \quad (53)$$

The cosmological constraints on the soft mass parameter $m_{1/2}$ are considered in the next Section.

Our results from the RG running from the high scale $\mathcal{O}(10^{13})$ GeV to the EW scale of $\mathcal{O}(10^2)$ GeV for the Higgs mass M_h as a function of m_0 and $m_{1/2}$ are given in Fig. 4.

As is clear from Fig. 4, the Higgs boson mass values derived from the running are compatible with the observed Higgs mass, while these values are robust against changes in the number of e-folds N and the gaugino mass scale $m_{1/2}$ for $m_{1/2} \leq m_0$. The prediction is controlled mainly by the top-quark pole mass M_t and the universal scalar mass m_0 that is fixed by the inflationary scale and equals the gravitino mass $m_{3/2}$. The explicit M_t dependence and the associated parametric uncertainties are presented in the next Section.

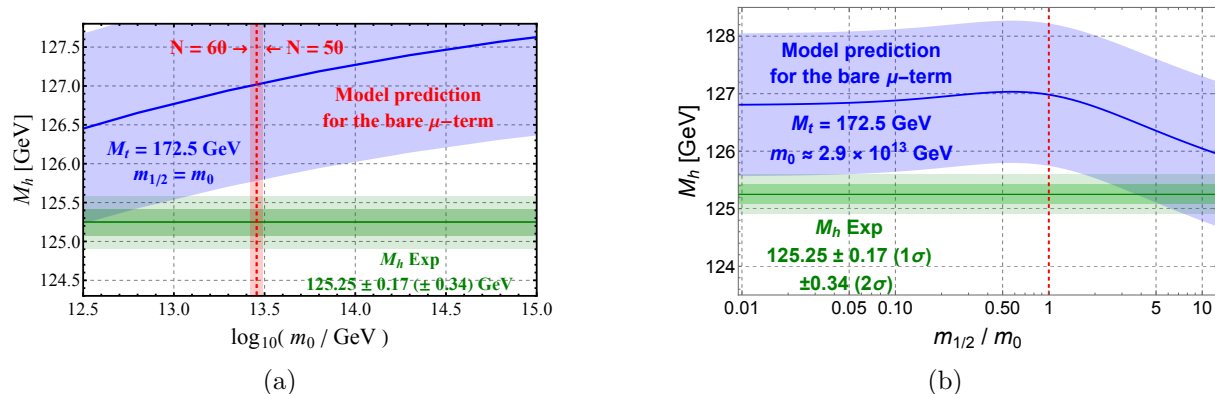


Figure 4: **(a)** The Higgs boson mass M_h as a function of the mass scale m_0 with the ATLAS+CMS combined top-quark mass $M_t = 172.5$ GeV [71] after assuming $m_{1/2} = m_0$. The red dashed line marks the model prediction for m_0 at $\gamma = 8/\sqrt{85}$ and $N = 55$, and the solid red line shows the stability bound for $\gamma = 0.17$. The shaded red vertical band shows the variation of the m_0 prediction for $N \in [50, 60]$. **(b)** M_h as a function of the mass parameter $m_{1/2}$ for $M_t = 172.5$ GeV and the scale m_0 fixed by $\gamma = 8/\sqrt{85}$ and $N = 55$. Both panels were obtained with **SusyHD**; the blue bands represent the intrinsic theory uncertainty, while the parametric uncertainty induced by $\alpha_s(M_Z)$ is not included.

We find that the Higgs boson mass rapidly approaches a plateau as $m_{1/2}$ decreases below m_0 and is effectively insensitive to $m_{1/2}$ throughout this region, as shown in Fig. 4(b). The leading logarithmic effect that could significantly alter the RG running of the quartic Higgs coupling λ is present only when both higgsinos and gauginos are light. In our framework, the higgsinos acquire masses of the order of the large scalar mass, and therefore decouple below the matching scale. Without light higgsinos in the EFT, the remaining light gauginos have no tree-level coupling to the Higgs boson, thus making their impact on the Higgs mass negligible. Consequently, as was also shown in Ref. [66], the SM alone is a reliable EFT well below the high scale m_0 . The entire information from the SUSY spectrum becomes encoded in the threshold corrections.

When the μ -term is dynamically generated by the superpotential interaction $\frac{\tilde{\lambda}}{M_{\text{P}}^{n-1}} \mathcal{S}^n H_u H_d$, the VEV $\langle \mathcal{S} \rangle = s_0 M_{\text{P}}$ at the end of inflation yields $\mu = \tilde{\lambda} s_0^n M_{\text{P}}$. In this case, the B -parameter differs

from that in Eq. (35) as

$$B = A - m_{3/2} + F^m \partial_m \ln \mu = A - m_{3/2} + n \frac{F^S}{S} = m_{3/2} \frac{(66 - 20n)s_0^2 + 44n - 48}{9(1 + 2s_0^2)}. \quad (54)$$

Given $n = 1$, the inequality $|B| \geq 2m_{3/2}$ is satisfied only when $|s_0| \geq \sqrt{2.2}$, which is incompatible with the positive gravitino mass condition $|s_0| < \sqrt{11/14}$. However, $n \geq 2$ is compatible with this condition, so we take $n = 2$.

Inserting Eq. (54) into the determinant condition in Eq. (45) yields

$$m_{3/2}^2 + A^2 = A \left(A - m_{3/2} + 2 \frac{F^S}{S} \right). \quad (55)$$

This can be rewritten as

$$866s_0^4 - 1429s_0^2 + 527 = 0 \quad (56)$$

that has two roots,

$$s_0^2 = \frac{1429 \pm \sqrt{216513}}{1732}. \quad (57)$$

Taking the positive sign gives $s_0 \approx 1.046$, which violates the positive gravitino mass condition and thus should be dismissed. Therefore, for $n = 2$, the vacuum state and the R-symmetry breaking parameter are fixed as

$$s_0 = \sqrt{\frac{1429 - \sqrt{216513}}{1732}} \approx 0.746, \quad \gamma = \frac{27\sqrt{33} + 101}{\sqrt{433(1429 - 81\sqrt{33})}} \approx 0.397. \quad (58)$$

Having fixed these parameters, the related gravitino mass for the middle value of e-folds $N = 55$ is given by

$$m_{3/2} \approx 7.7 \times 10^{13} \text{ GeV} \quad (59)$$

and differs from that in Eq. (52).

Accordingly, the boundary conditions for RG running are also different, being given by

$$\tan \beta = 1, \quad m_0 = m_{3/2}, \quad A = \mu_{\text{eff}} = \frac{m_{3/2}}{8} (9 - \sqrt{33}), \quad B = \frac{m_{3/2}}{24} (63 + \sqrt{33}). \quad (60)$$

The expression for μ_{eff} fixes the coupling constant $\tilde{\lambda}$ as

$$\tilde{\lambda} = \frac{9 - \sqrt{33}}{3} (1 + 2s_0^2) \frac{m}{M_{\text{P}}} = 36 \sqrt{\frac{6(3431 - 549\sqrt{33})}{228191}} \frac{m}{s_0 M_{\text{P}}} \approx 2.26 \times 10^{-5}. \quad (61)$$

Figure 5 illustrates the RG running obtained with the dynamically generated μ -term. The higher scale of the gravitino mass lifts the predicted Higgs mass in the plateau region where $m_{1/2} < m_0$ relative to Fig. 4. Nevertheless, as $m_{1/2}$ approaches m_0 , the dynamical scenario has better agreement with the measured Higgs boson mass.

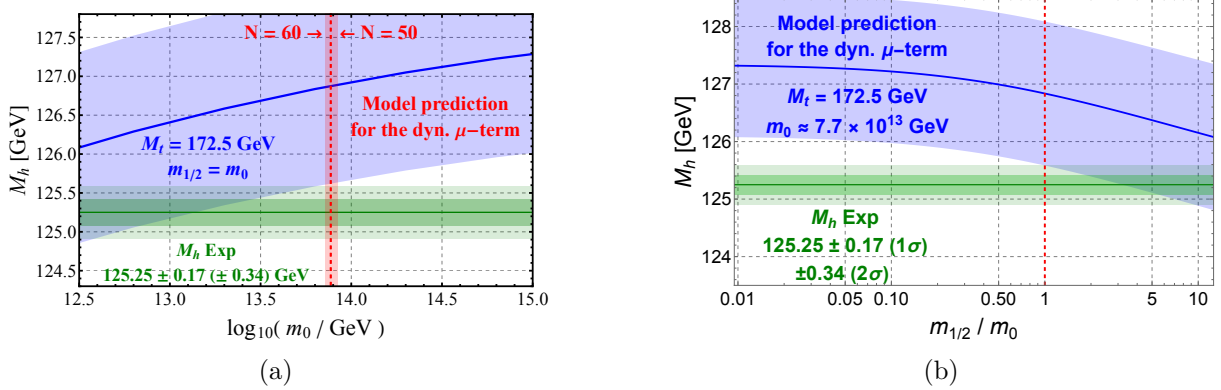


Figure 5: **(a)** The Higgs boson mass M_h as a function of the mass scale m_0 with the ATLAS+CMS combined top-quark mass $M_t = 172.5$ GeV [71] after assuming $m_{1/2} = m_0$. The red dashed line marks the model prediction for m_0 at $\gamma \approx 0.397$ and $N = 55$. The shaded red vertical band shows the variation of the m_0 prediction for $N \in [50, 60]$. **(b)** M_h as a function of the mass parameter $m_{1/2}$ for $M_t = 172.5$ GeV and the scale m_0 fixed by $\gamma \approx 0.397$ and $N = 55$. Both panels were obtained with `SusyHD`; the blue bands represent the intrinsic theory uncertainty, while the parametric uncertainty induced by $\alpha_s(M_Z)$ is not included.

6 Anomaly mediation of SUSY breaking and wino dark matter

The gaugino masses M_a are generated by the hidden sector F -terms, requiring a specification of the gauge kinetic function f_a which is not fixed by Starobinsky supergravity alone.

First, consider a constant gauge kinetic function, $f_a = 1$. In this case, Eq. (37) implies that the tree-level contributions vanish, $M_a^{\text{tree}} = 0$. Consequently, non-vanishing gaugino masses can only arise from quantum corrections via the super-Weyl anomaly. This mechanism is known as anomaly-mediated supersymmetry breaking (AMSB) [72–74]. It yields gaugino masses proportional to the gravitino mass and the beta-functions of the corresponding gauge groups as

$$M_a^{\text{AMSB}} = \frac{\beta(g_a)}{g_a} m_{3/2} = \frac{b_a \alpha_a}{4\pi} m_{3/2}, \quad (62)$$

where $a = 1, 2, 3$ denotes the $U(1)_Y$, $SU(2)_L$, and $SU(3)_C$ gauge groups of the SM, $\alpha_a = g_a^2/(4\pi)$ are the fine-structure constants, and b_a are the one-loop beta-function coefficients. For the MSSM, $b_a = (33/5, 1, -3)$, we have

$$M_1^{\text{AMSB}} = \frac{33/5 \cdot \alpha_1}{4\pi} m_{3/2}, \quad M_2^{\text{AMSB}} = \frac{1 \cdot \alpha_2}{4\pi} m_{3/2}, \quad M_3^{\text{AMSB}} = \frac{-3 \cdot \alpha_3}{4\pi} m_{3/2}. \quad (63)$$

At the high-energy matching scale $m_0 = m_{3/2}$, the gauge couplings $\alpha_a(m_0)$ are evaluated via RG evolution. In our case this typically yields $\alpha_a(\tilde{m}) \sim 0.023\text{--}0.027$. This variation is small enough that the AMSB mass hierarchy is primarily determined by the beta-function coefficients, enforcing $|M_1^{\text{AMSB}}| > |M_3^{\text{AMSB}}| > |M_2^{\text{AMSB}}|$.

The total gaugino mass is a sum of the tree-level contribution, determined by the gauge kinetic function f_a in Eq. (38), and the quantum AMSB contribution:

$$M_a^{\text{total}} = M_a^{\text{tree}} + M_a^{\text{AMSB}}. \quad (64)$$

The high-scale spectrum strongly restricts the neutralino LSP. Higgsinos are heavy because $|\mu_{\text{eff}}| \sim m_{3/2}$, while nearly pure binos annihilate inefficiently once sfermions and higgsinos are

decoupled, but this would overproduce DM in the minimal thermal history. Instead, a nearly pure wino retains unsuppressed $SU(2)_L$ annihilation and chargino–neutralino co-annihilation. Non-minimal bino scenarios requiring co-annihilation, resonant annihilation, late entropy dilution or R -parity violation are outside the scope of this investigation. Therefore, we focus on the wino LSP branch. Since the tree-level contribution in Eq. (38) is universal, the relative splittings amongst the total gaugino masses are controlled by the AMSB contribution. The wino branch is realised by choosing the universal tree-level contribution, so that it cancels most of the AMSB contribution to M_2 , leaving TeV-scale winos, while binos and gluinos remain much heavier. Constraints on M_a^{total} can be inferred from the Higgs boson mass running in Figs. 4(b) and 5(b), but a stronger restriction comes from cosmology: the thermal relic density condition fixes the physical wino mass as shown below.

In our setup, the MSSM scalars are lighter than the inflaton, with $m_{\text{inf}}/m_0 \approx 1.1$ for the bare μ -term scenario. Consequently, these scalars can be efficiently produced by gravitational particle production at the end of inflation [75]. Following Ref. [76], the present-day energy density of particular gravitationally produced scalar species, normalised by the entropy density s , scales as

$$\frac{\rho_0^{(\text{GP})}}{s} \sim \frac{\mathcal{C}}{4} \frac{m_0 H_{\text{inf}} T_{\text{R}}}{M_{\text{P}}^2} \simeq 4 \times 10^{-10} \text{ GeV} \cdot \mathcal{C} \left(\frac{m_0}{10^9 \text{ GeV}} \right) \left(\frac{H_{\text{inf}}}{10^9 \text{ GeV}} \right) \left(\frac{T_{\text{R}}}{10^{10} \text{ GeV}} \right). \quad (65)$$

Here $\mathcal{C} \sim 10^{-2}$ and T_{R} is the reheating temperature, typically of the order 10^8 – 10^9 GeV [21]. With $H_{\text{inf}} \sim \mathcal{O}(10^{13})$ GeV and $m_0 \sim \mathcal{O}(10^{13})$ GeV, this estimate implies that a stable scalar population can exceed the observed DM abundance by many orders of magnitude. The precise abundance depends on a production coefficient, a reheating history and a number of gravitationally produced species.

Avoiding the scalar overproduction requires the gravitationally produced scalars to be unstable. A possible way to realise that is to make wino the LSP, so that the heavy scalars decay into final states containing winos. In that case the scalar overabundance is not automatically inherited by the wino LSP. Neglecting subsequent wino annihilation and entropy dilution, the injected wino yield is schematically given by

$$Y_{\tilde{W}}^{\text{inj}} \sim N_{\tilde{W}} \text{Br}(\phi \rightarrow \tilde{W} + X) \frac{\rho_{\phi}^{(\text{GP})}}{m_0 s}, \quad (66)$$

where $N_{\tilde{W}}$ is the average number of winos produced per scalar decay and $\text{Br}(\phi \rightarrow \tilde{W} + X)$ denotes the relevant branching fraction. The corresponding relic abundance is then estimated as

$$\Omega_{\tilde{W}} h^2 \sim \frac{M_2}{m_0} N_{\tilde{W}} \text{Br}(\phi \rightarrow \tilde{W} + X) \frac{\rho_{\phi}^{(\text{GP})}}{s} \frac{s_{\text{today}}}{\rho_c/h^2}. \quad (67)$$

Hence, lowering the ratio M_2/m_0 can reduce the final energy density transferred to the wino LSP. However, this estimate is not sufficient to determine the final relic abundance. In the non-thermal regime

$$m_0 > M_2 > T_{\text{R}}, \quad (68)$$

thermal wino production is Boltzmann suppressed, and the final abundance depends on the post-inflationary history, including the scalar yield, decay temperature, branching ratios and multiplicities, possible wino annihilation after injection, and any late-time entropy dilution. A reliable assessment of this branch therefore requires a dedicated calculation, which we leave for future work.

A qualitatively different possibility is to lower the gaugino masses so that the wino mass lies well below the reheating temperature, $M_2 \ll T_{\text{R}}$. In this thermal regime, the unsuppressed $SU(2)_L$ gauge interactions efficiently bring winos into chemical and kinetic equilibrium with the SM

plasma. The final relic abundance is then determined by standard thermal freeze-out and is insensitive to the initial gravitational-production yield [73]. This should be distinguished from the non-thermal regime $M_2 > T_R$, where the final abundance depends on the post-inflationary history, including gravitational production, decay chains, possible annihilation after injection, and entropy dilution.

This corresponds to the thermal “wino miracle” scenario. For a pure wino, the neutral and charged components form an almost degenerate $SU(2)_L$ multiplet, so co-annihilation with the charged wino states is essential in the relic density calculation. In addition, for TeV-scale electroweak multiplets the exchange of electroweak gauge bosons generates a long-range potential between the slowly moving annihilating particles. The resulting Sommerfeld enhancement substantially increases the effective annihilation cross section at freeze-out [77–80]. Established calculations including these effects place the thermal wino mass at about 2.7–3.0 TeV, with a mild dependence on higher-order electroweak corrections and possible departures from the pure-wino limit [77, 80, 81]. We therefore adopt $M_2 \simeq 3$ TeV as the thermal target and do not recalculate the freeze-out abundance in this work.

Direct detection constraints are also mild for the pure wino limit realised here. Since the Higgsino mass parameter is of the order of the high SUSY-breaking scale, $\mu \sim 10^{13}$ GeV, the Higgsino admixture of the neutral wino is suppressed by m_W/μ and the tree-level Higgs-mediated spin-independent scattering amplitude is negligible. The tree-level Z -exchange contribution is absent for a Majorana neutral wino. The leading spin-independent scattering therefore arises from EW loop effects. One-loop diagrams generate effective couplings of the wino to quarks and to the Higgs sector, while the effective coupling to gluons first appears at two loops and gives an important contribution to the nucleon matrix element [82–84]. For a nearly pure TeV-scale wino, the spin-independent wino-proton cross section is only weakly dependent on the wino mass and is predicted to be

$$\sigma_{\text{SI}}^p \simeq 2.3 \times 10^{-47} \text{ cm}^2 \quad (69)$$

with an uncertainty of the order (30–40)% from perturbative and hadronic inputs [84]. This value is below current LZ bounds for multi-TeV dark matter, but it lies above the irreducible neutrino background and is within the target range of next-generation multi-ton liquid-xenon experiments such as DARWIN/XLZD [85–87]. Therefore, present direct detection data do not exclude the pure wino DM scenario considered here, while next-generation multi-ton liquid-xenon experiments will directly probe this parameter region.

To illustrate how $M_2 \approx 3$ TeV can be realized in our approach, we first evaluate the AMSB contributions. For the bare μ -term case with $m_{3/2} \approx 2.86 \times 10^{13}$ GeV, we find

$$M_1^{\text{AMSB}} \approx 3.60 \times 10^{11} \text{ GeV}, \quad M_2^{\text{AMSB}} \approx 5.98 \times 10^{10} \text{ GeV}, \quad M_3^{\text{AMSB}} \approx -1.87 \times 10^{11} \text{ GeV}. \quad (70)$$

For the dynamically generated μ -term case with $m_{3/2} \approx 7.70 \times 10^{13}$ GeV, we obtain

$$M_1^{\text{AMSB}} \approx 9.85 \times 10^{11} \text{ GeV}, \quad M_2^{\text{AMSB}} \approx 1.60 \times 10^{11} \text{ GeV}, \quad M_3^{\text{AMSB}} \approx -4.90 \times 10^{11} \text{ GeV}. \quad (71)$$

Therefore, to obtain $M_2^{\text{total}} \approx 3$ TeV, the universal tree-level gaugino mass must be fixed to $M_a^{\text{tree}} \approx -5.97 \times 10^{10}$ GeV for the bare μ -term case, and $M_a^{\text{tree}} \approx -1.59 \times 10^{11}$ GeV for the dynamically generated μ -term case. This yields the following total gaugino mass spectra at the high scale:

For the bare μ -term case, we have

$$M_1^{\text{total}} \approx 3 \times 10^{11} \text{ GeV}, \quad M_2^{\text{total}} \approx 1.59 \times 10^3 \text{ GeV}, \quad M_3^{\text{total}} \approx -2.47 \times 10^{11} \text{ GeV}. \quad (72)$$

For the dynamically generated μ -term case, we have

$$M_1^{\text{total}} \approx 8.25 \times 10^{11} \text{ GeV}, \quad M_2^{\text{total}} \approx 1.55 \times 10^3 \text{ GeV}, \quad M_3^{\text{total}} \approx -6.49 \times 10^{11} \text{ GeV}. \quad (73)$$

In both cases, the wino mass M_2^{total} is fixed at the matching scale m_0 and runs downwards to yield $M_2 \approx 3$ TeV at the low-energy scale. We calculate the Higgs mass with two independent EFT implementations: SusyHD [66]³ and HSSUSY within FlexibleSUSY [67,68]. Both packages match the MSSM directly onto the SM at the high SUSY scale and re-sum the large logarithms generated by the separation between this scale and the electroweak scale. We use SusyHD for the main numerical analysis and HSSUSY as an independent cross-check of the Higgs mass predictions and their uncertainty estimates.

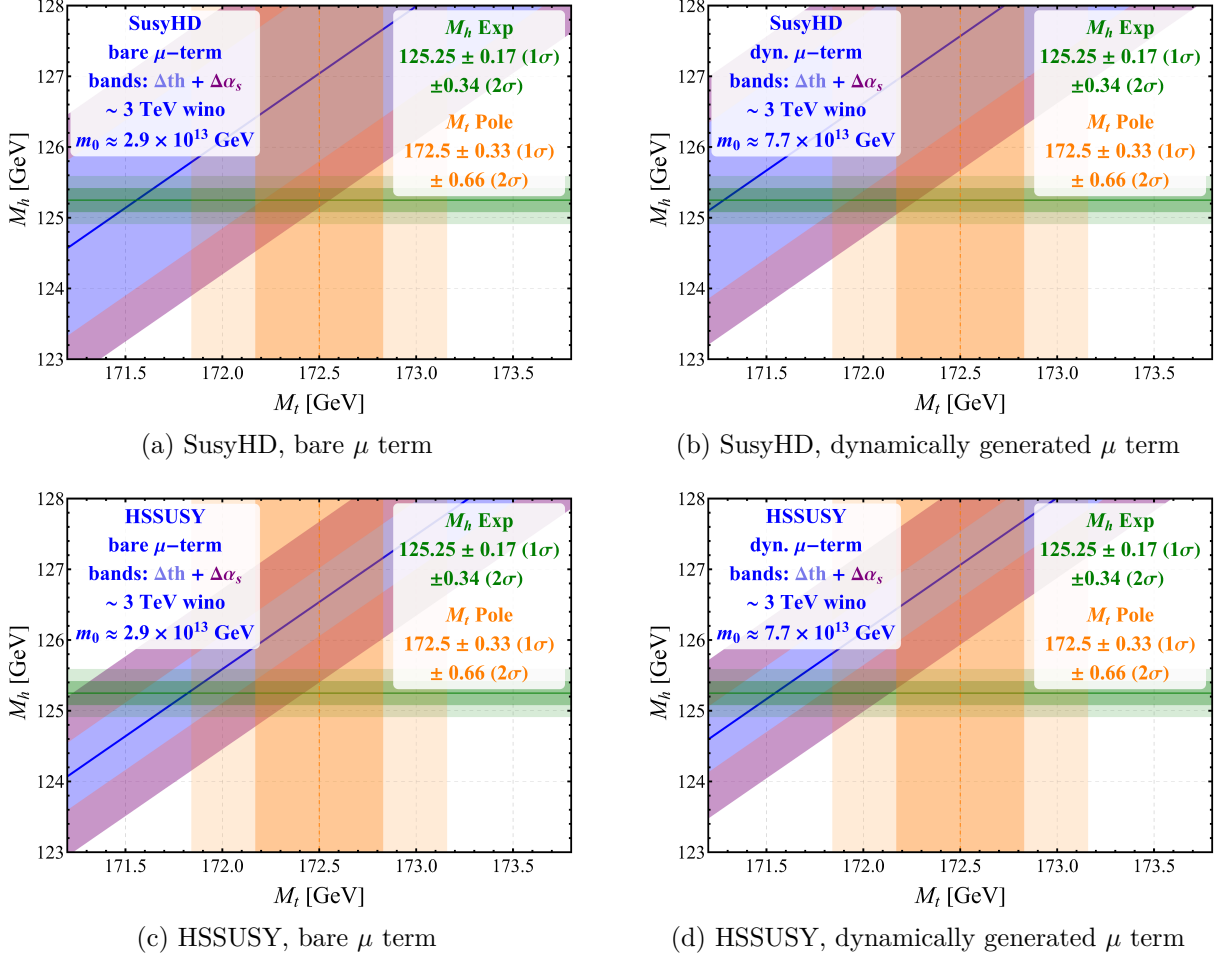


Figure 6: Higgs boson mass M_h as a function of the ATLAS+CMS combined top-quark pole mass M_t [71]. Panels (a) and (c) correspond to the bare- μ scenario with $\gamma = 8/\sqrt{85}$, while panels (b) and (d) correspond to the dynamically generated μ scenario with $\gamma \simeq 0.397$. In all panels, the high-scale total gaugino masses are chosen so that RG evolution gives a physical low-energy wino mass $M_2 \simeq 3$ TeV. The green shaded regions show the 1σ and 2σ experimental constraints on M_h , while the orange shaded regions show the corresponding constraints on M_t from the Particle Data Group (PDG) 2024 [88]. The blue bands show the intrinsic theory uncertainty $\Delta_{\text{th}} M_h$, while the purple extensions show the additional parametric uncertainty induced by $\alpha_s(M_Z)$. The two uncertainties are displayed additively for visual comparison but are quoted separately in the text.

³While comparing SusyHD and HSSUSY predictions, we have found the bug in SusyHD: the fast-interpolation table distributed with SusyHD v1.0.2 was independent of its g_3 coordinate and therefore missed part of the α_s dependence. We regenerated the table with the correct g_3 boundary condition and used this local corrected version throughout the analysis. The correction leaves the central Higgs masses and intrinsic SusyHD theory uncertainties unchanged at the quoted precision, but restores the correct α_s uncertainty. Appendix A gives the complete comparison, explains the uncertainty prescriptions and documents the correction. The corrected SusyHD source, regenerated table, regeneration script and README file are provided as supplementary material.

We find that both EFT implementations give a Higgs boson mass compatible with the measured value after imposing the thermal wino condition. With the central input values $M_t = 172.52$ GeV and $\alpha_s(M_Z) = 0.1180$, we obtain

$$\begin{aligned}
M_h^{\text{SusyHD}}(\text{bare } \mu) &= 127.08 \pm 1.24_{\text{th}} \pm 0.65_{\alpha_s} \text{ GeV}, \\
M_h^{\text{HSSUSY}}(\text{bare } \mu) &= 126.58 \pm 0.48_{\text{th}} \pm 0.65_{\alpha_s} \text{ GeV}, \\
M_h^{\text{SusyHD}}(\text{dynamical } \mu) &= 127.61 \pm 1.24_{\text{th}} \pm 0.65_{\alpha_s} \text{ GeV}, \\
M_h^{\text{HSSUSY}}(\text{dynamical } \mu) &= 127.10 \pm 0.47_{\text{th}} \pm 0.66_{\alpha_s} \text{ GeV}.
\end{aligned}
\tag{74}$$

The SusyHD and HSSUSY central predictions differ by about 0.5 GeV for both the bare and dynamical μ scenarios, and are consistent within the quoted theory and parametric uncertainties.

The two quoted errors have different origins. The theory error estimates the missing higher-order contributions. SusyHD provides separate low-energy SM, high-scale SUSY-matching and power-suppressed EFT components, which we combine linearly. For the bare μ case, this gives

$$\Delta_{\text{th}} M_h^{\text{SusyHD}} = 1.2389 + 0.0009 + 0.0006 = 1.2404 \text{ GeV},
\tag{75}$$

while for the dynamically generated μ case, we get

$$\Delta_{\text{th}} M_h^{\text{SusyHD}} = 1.2387 + 0.0026 + 0.0005 = 1.2418 \text{ GeV}.
\tag{76}$$

Therefore, the SusyHD theory error is almost entirely the low-energy SM component dominated by missing higher-order terms in the extraction of the running top Yukawa coupling and in the conversion of the running Higgs quartic coupling into the Higgs pole mass. HSSUSY uses a more recent prescription based on variations of the higher-order terms entering the extraction of the running top Yukawa coupling, the renormalisation scale in the Higgs pole mass calculation and the high-scale matching. It gives theory uncertainties of 0.4820 GeV and 0.4713 GeV for the bare and dynamically generated μ cases, respectively. The different theory errors therefore reflect different uncertainty prescriptions rather than a disagreement between the central predictions [89].

The α_s error is parametric. Varying $\alpha_s(M_Z) = 0.1180 \pm 0.0009$ changes the QCD conversion of the top pole mass into the running top Yukawa coupling and, hence, the RG evolution of y_t and λ over the large interval between the electroweak and SUSY scales. The resulting uncertainties are 0.6518 GeV and 0.6546 GeV in SusyHD, and 0.6545 GeV and 0.6573 GeV in HSSUSY, for the bare and dynamically generated μ scenarios, respectively. At fixed M_t , we add the theory and α_s uncertainties linearly, giving total vertical uncertainties of 1.89 GeV and 1.14 GeV for the bare- μ SusyHD and HSSUSY results, and 1.90 GeV and 1.13 GeV for the corresponding dynamical- μ results. This linear sum is a conservative uncertainty envelope, not a statistical confidence interval. The top-mass uncertainty, $\Delta_{M_t} M_h \simeq 0.63$ GeV, is kept separate because M_t is varied explicitly along the horizontal axis in Fig. 6.

The resulting thermal wino scenario is sharply predictive at future colliders. The robustness of this prediction originates from the highly hierarchical SUSY spectrum realised in our framework. The Higgsino mass parameter, together with the bino and gluino masses, resides at the scale μ , $M_1, M_3 \sim 10^{11}\text{--}10^{13}$ GeV, whereas the wino mass is of the order $M_2 \simeq 3$ TeV. The chargino mass matrix contains off-diagonal entries of order m_W , while the Higgsino mass parameter is near the high supersymmetry-breaking scale. Consequently, the Higgsino admixture in the light chargino and neutralino eigenstates is suppressed by m_W/μ , and the corresponding mass corrections are negligible. The lightest chargino and neutralino are therefore effectively pure wino states.

Since the charged and neutral winos belong to the same $SU(2)_L$ multiplet, they are degenerate at tree level in the pure-wino limit. Two-loop electroweak corrections generate a mass splitting

of about 160–165 MeV for a multi-TeV wino, giving a chargino lifetime of approximately 0.2 ns and, hence,

$$c\tau \simeq 6 \text{ cm.}$$

The dominant decay is $\tilde{\chi}_1^\pm \rightarrow \tilde{\chi}_1^0 \pi^\pm$, and the pion is usually too soft to be reconstructed [90]. In the laboratory frame, the mean flight distance is $\beta\gamma c\tau$, so boosted charginos can cross several inner tracking layers before decaying and produce a reconstructable disappearing track. The physical lifetime of 0.2 ns is somewhat shorter than the lifetime near 1 ns for which the ATLAS sensitivity is maximal, because a larger fraction of the longer-lived charginos leave enough inner-layer hits. Nevertheless, it is well within the effective search region. Using tracklets reconstructed from three or four innermost-layer measurements, the latest ATLAS analysis excludes the theoretical pure-wino line up to about 670 GeV; allowing the lifetime to vary, the strongest observed wino limit is about 880 GeV near 1 ns [91].

At the HL-LHC, with $\sqrt{s} = 14 \text{ TeV}$ and 3 ab^{-1} , the ATLAS disappearing-track projection gives a 5σ discovery reach of about 0.8 TeV and a 95% confidence-level exclusion reach of about 1.1 TeV for a pure wino [92]. The much larger data set will therefore extend the present sensitivity substantially, but the limited centre-of-mass energy prevents the HL-LHC from reaching the thermal wino mass. The HL-LHC will provide an important indirect test of the scenario through improved precision on the SM inputs entering the Higgs mass prediction. The combined ATLAS+CMS HL-LHC projection gives an expected Higgs boson mass uncertainty of about 21 MeV, while the top-quark mass uncertainty could reach about 200 MeV in optimistic profiled analyses, with more conservative projections at the few-hundred-MeV level [93, 94]. Since the predicted Higgs mass in our framework is sensitive to M_t and the high-scale threshold corrections fixed by the SUSY-breaking sector, those measurements will significantly reduce the allowed parameter space and provide a complementary indirect probe of our scenario.

A future 100 TeV proton collider changes the situation qualitatively. Dedicated disappearing-track studies show that its discovery reach extends beyond the thermal wino mass scale, $m_{\tilde{\chi}_1^\pm} \simeq m_{\tilde{\chi}_1^0} \simeq 3 \text{ TeV}$, for tracker configurations optimised for short charged-particle tracks [95]. Therefore, the 3 TeV wino predicted in this scenario lies within the projected discovery reach of such a collider. A 100 TeV proton collider can discover the disappearing-track signal from a 3 TeV wino or fully exclude this minimal pure wino DM scenario.

7 Conclusion

In this paper, we proposed a framework connecting cosmic inflation and CMB observables to particle physics phenomenology at colliders and direct detection experiments, with SUSY providing the link between them. In our approach, the hidden sector is not introduced *ad hoc* but emerges from the dual description of the Starobinsky supergravity that gravitationally couples to the MSSM in the Einstein frame. Inflation is realised in the bosonic part of the hidden sector and leads to a Minkowski vacuum with a non-vanishing VEV s_0 of the real scalar component of the goldstino superfield \mathcal{S} .

The inflation sector is effectively controlled by two parameters, the mass parameter m and the vacuum expectation value s_0 . The parameter m is fixed by the CMB amplitude of the scalar power spectrum and the number of e-folds between horizon crossing at the pivot scale and the end of inflation. The non-vanishing s_0 triggers spontaneous SUSY breaking, with the gravitino mass $m_{3/2}$ determined by m and s_0 . The upper bound on s_0 follows from positivity of $m_{3/2}^2$, whereas the lower bound arises from forbidding inflaton decays into two gravitini, $m_{\text{inf}} < 2m_{3/2}$, in order to avoid gravitino overproduction. Within the allowed interval of s_0 , the inflationary dynamics is effectively of the single-field type. The predicted scalar tilt n_s is slightly larger than

that in the original Starobinsky model, thus improving agreement with the recent ACT-preferred data.

Spontaneous SUSY breaking is gravitationally mediated to the MSSM, whose soft parameters are derived in terms of $m_{3/2}$ and s_0 . The same hidden sector can also generate a high-scale Higgs sector μ term. In particular, the coupling $\mathcal{S}^2 H_u H_d$ can realise a singlet-generated μ mechanism, where the singlet is identified with the goldstino superfield already present in Starobinsky supergravity. Hence, no additional singlet has to be introduced “by hand”. We also considered the case in which the MSSM contains a bare μ term independent of the hidden sector.

To connect the resulting MSSM spectrum to SM phenomenology, we demand the existence of a light SM Higgs doublet. This implies that the determinant of the Higgs-sector mass-squared matrix should vanish at the high scale, $\det(\mathcal{M}_H^2) = 0$. With minimal stop mixing, this gives an equation on s_0 . Its solution fixes the inflationary predictions, the gravitino mass and the soft parameters, except for the gaugino masses because the gauge kinetic function is not specified by Starobinsky supergravity alone. Instead, the gaugino sector is constrained by the post-inflationary and DM phenomenology.

With conserved R -parity, the LSP is stable and can constitute DM. Since the MSSM scalars are lighter than the inflaton, they can be gravitationally produced after inflation. Depending on the reheating history and scalar’s stability, their population can exceed the observed DM abundance. A minimal way to avoid a stable heavy-scalar relic is to realise a gaugino LSP. After including anomaly-mediated contributions, the LSP can be a wino. The wino DM can be either non-thermal or thermal. A reliable calculation of the non-thermal abundance requires a detailed treatment of reheating, heavy-particle decays, subsequent annihilation and possible entropy production, which we leave for future work. In the thermal branch, the wino is nearly pure and the observed relic abundance selects a physical mass of 2.7–3.0 TeV. This branch requires a high-precision cancellation between the universal tree-level contribution to M_2 and the anomaly-mediated contribution, and is therefore significantly fine-tuned.

The resulting spectrum with scalar superpartners and higgsinos near the inflationary scale and a TeV-scale wino LSP is characteristic of split-SUSY scenarios [96]. The soft terms determine the high-scale threshold corrections and the boundary condition for the RG evolution of the Higgs quartic coupling, while its tree-level MSSM contribution vanishes for $\tan\beta = 1$. Three-loop RG evolution down to the top-quark mass scale gives a Higgs boson mass compatible with experiment. Independent calculations with `SusyHD` and `HSSUSY` agree on the central prediction at the level of about 0.5 GeV. We quote the intrinsic theory uncertainty separately from the parametric uncertainty induced by $\alpha_s(M_Z)$ and adopt the more recent `HSSUSY` estimate for the residual perturbative uncertainty. This establishes the link between the CMB normalisation, the scale of SUSY breaking and the Higgs-boson mass. The predicted Higgs mass depends only weakly on the number of e-folds and becomes effectively insensitive to $m_{1/2}$ once $m_{1/2} < m_0$.

The thermal wino target remains beyond the reach of the HL-LHC. For $\sqrt{s} = 14$ TeV and 3 ab^{-1} , disappearing-track projections give a discovery reach of about 0.8 TeV and an exclusion reach of about 1.1 TeV for a pure wino [92]. The HL-LHC will therefore substantially extend the current sensitivity, but it will not reach the 2.7–3.0 TeV thermal mass. A future 100 TeV proton collider can directly probe this full target through the disappearing-track signature.

The thermal wino in our scenario is compatible with existing direct detection bounds. Tree-level spin-independent scattering is suppressed by the very heavy higgsino mass, while the loop-induced wino-nucleon cross section lies below current sensitivities but within the projected reach of next-generation multi-ton liquid-xenon detectors. Electroweak radiative corrections split the charged and neutral winos by about 160 MeV, producing a chargino lifetime of about 0.2 ns and the characteristic disappearing-track signature. Current LHC searches already probe this lifetime

regime. Direct detection and future disappearing-track searches will provide complementary tests of the same thermal wino branch.

The same strategy can be applied to other realisations of inflation and SUSY breaking in supergravity. Different Kähler potentials and superpotentials lead to different soft terms and, hence, different high-scale boundary conditions for RG evolution. One may also consider coupling Starobinsky supergravity to the MSSM in the Jordan frame or generating the μ term through a combination of bare and dynamical contributions. The master f -function can be modified to allow primordial black hole production, providing an additional non-particle DM candidate [97, 98].

Our framework can naturally accommodate neutrino masses through an embedding of the visible sector into a supersymmetric $SO(10)$ grand unified theory. In this case, each matter generation, including a right-handed neutrino, is contained in a single 16-plet representation, while $B - L$ breaking generates light neutrino masses through the type-I see-saw mechanism [99, 100]. Leptogenesis can also be included, while its detailed realisation requires specifying the GUT-breaking and flavour sectors. We leave reheating and non-thermal wino DM for future work.

In summary, we constructed a specific framework linking the CMB normalisation, high-scale SUSY breaking, Higgs mass generation and TeV-scale DM phenomenology. The inflation input fixes the characteristic high-energy scale, whereas the resulting low-energy spectrum gives testable predictions for direct detection and disappearing-track searches.

Acknowledgements

The authors are grateful to Constantinos Pallis, Roman Pasechnik, Antonio Morais, Anca Preda and Tomislav Prokopec for discussions and correspondence.

The work of DF was funded by the NWA ORC programme Emergence at All Scales. DF was also partially supported by the Foundation for Advancement of Theoretical Physics and Mathematics "BASIS". AB is supported in part through the NExT Institute and STFC CG ST/X000583/1. AB acknowledges partial support from Leverhulme Trust project MONDMag (RPG-2022-57). SVK was partially supported by the Simons Foundation in the USA, and the World Premier International Research Center Initiative, MEXT, Japan. DF and SVK were partially supported by Tomsk State University where this investigation was initiated under the development program Priority-2030. SVK is grateful to the International Institute of Physics in Natal, Brazil, for the kind hospitality extended to him during this investigation.

A Higgs mass uncertainties, and comparison of SusyHD and HSSUSY

SusyHD provides three components of its intrinsic theory uncertainty: a low-energy SM component, an MSSM-to-SM matching component, and an EFT truncation component. Combining them linearly gives

$$\Delta_{\text{th}} M_h^{\text{SusyHD}} = 1.24 \text{ GeV} \quad (1)$$

for both the bare and dynamically generated μ cases. The uncertainty is dominated by the low-energy SM component; the SUSY-matching and EFT truncation components are numerically negligible at this precision.

HSSUSY uses a more recent uncertainty prescription. Its low-energy component is estimated by varying the treatment of higher-order corrections in the extraction of the running top Yukawa coupling and by varying the renormalisation scale used in the Higgs pole mass calculation, while

the high-scale matching uncertainty is evaluated separately. For those two cases, HSSUSY gives

$$\Delta_{\text{th}} M_h^{\text{HSSUSY}} = 0.482 \text{ GeV} \quad \text{and} \quad 0.471 \text{ GeV}, \quad (2)$$

respectively. The difference between the **SusyHD** and HSSUSY theory uncertainties reflects different perturbative uncertainty prescriptions, not a disagreement between their central predictions.

During the comparison, we found a bug in the precomputed fast interpolation table distributed with **SusyHD**, v1.0.2. The table is parametrised by the strong gauge coupling g_3 at the top-mass scale, but its entries are numerically independent of this coordinate. In the original table generation, the RG boundary condition used the fixed central value $g_{3\text{MT}}$ rather than the varying grid value $g_{3\text{MT}}^{\text{var}}$. As a result, a variation of $\alpha_s(M_Z)$ was propagated through the top Yukawa coupling, but its independent effect through g_3 was omitted, leading to an underestimated α_s parametric uncertainty.

We regenerated the interpolation table using the original **SusyHD** RG equations and the corrected boundary condition

$$g_3(0) = g_{3\text{MT}}^{\text{var}}. \quad (3)$$

The resulting table has a non-zero dependence on g_3 . We use this table in a local corrected version, **SusyHD**, v1.0.3 (30 June 2026). This is not an official upstream **SusyHD** release. The corrected source, the regenerated table, the regeneration script and a README file are provided as supplementary material. The public **SusyHD** interface and all input conventions are unchanged.

With the corrected table, the α_s uncertainties in **SusyHD** are

$$\Delta_{\alpha_s} M_h^{\text{SusyHD}} = 0.652 \text{ GeV} \quad \text{and} \quad 0.655 \text{ GeV} \quad (4)$$

for the bare and dynamically generated μ cases, respectively. HSSUSY gives

$$\Delta_{\alpha_s} M_h^{\text{HSSUSY}} = 0.654 \text{ GeV} \quad \text{and} \quad 0.657 \text{ GeV}, \quad (5)$$

respectively. The corrected **SusyHD** and HSSUSY calculations give almost identical α_s dependence. The correction leaves the central **SusyHD** masses and intrinsic theory uncertainties unchanged at the quoted precision because the central g_3 grid point was already evaluated correctly.

The Higgs mass calculation involves boundary conditions imposed at two widely separated scales. The measured top pole mass, the strong coupling and the remaining EW inputs are converted into running SM parameters at a low renormalisation scale. In particular, one has

$$M_t^{\text{pole}} \longrightarrow m_t^{\overline{\text{MS}}}(Q_{\text{EW}}) \longrightarrow y_t(Q_{\text{EW}}). \quad (6)$$

The gauge and Yukawa couplings are evolved to the scale m_0 where the MSSM-to-SM matching condition fixes the boundary value of the SM Higgs quartic coupling as

$$\lambda(m_0) = \frac{1}{4} \left[g_2^2(m_0) + \frac{3}{5} g_1^2(m_0) \right] \cos^2 2\beta + \Delta\lambda(m_0). \quad (7)$$

For $\tan\beta = 1$,

$$\cos 2\beta = 0, \quad (8)$$

so the tree-level contribution vanishes and

$$\lambda(m_0) = \Delta\lambda(m_0). \quad (9)$$

The quartic coupling and the other SM parameters are evolved to the EW scale, where the running parameters are converted into the physical Higgs pole mass.

The coupled low- and high-scale boundary conditions are solved iteratively. Iteration removes numerical inconsistencies in the boundary-value solution, but it does not remove the uncertainty due to missing perturbative orders. The relation between the measured top pole mass and the running top mass is known only as a truncated perturbative expansion,

$$M_t^{\text{pole}} = m_t^{\overline{\text{MS}}}(Q) \left[1 + \Delta_t^{(1)}(Q) + \Delta_t^{(2)}(Q) + \Delta_t^{(3)}(Q) + \dots \right] \quad (10)$$

Different prescriptions that are equivalent up to the known order can therefore give slightly different values of $y_t(Q_{\text{EW}})$ after convergence.

The top Yukawa coupling strongly affects the RG evolution of the Higgs quartic coupling. Schematically one has,

$$\beta_\lambda \supset -\frac{6y_t^4}{16\pi^2} + \frac{12\lambda y_t^2}{16\pi^2} + \dots \quad (11)$$

Consequently, a small higher-order difference in the extraction of $y_t(Q_{\text{EW}})$ changes the evolution of λ over the large interval

$$\ln\left(\frac{m_0}{M_t}\right) \simeq 25. \quad (12)$$

The RG evolution does not introduce an independent source of uncertainty. Instead, the long running interval increases the sensitivity of the predicted low-energy Higgs mass to missing higher-order terms in the low-energy determination of y_t and in the conversion between the running quartic coupling and the Higgs pole mass.

The intrinsic perturbative uncertainty should be distinguished from the parametric uncertainty induced by the experimental errors of the SM inputs. Varying

$$M_t = 172.52 \pm 0.33 \text{ GeV} \quad (13)$$

induces $\Delta_{M_t} M_h \simeq 0.627 \text{ GeV}$ in both codes and for both cases. The M_t uncertainty is kept separate in the present analysis because the dependence on M_t is explicitly displayed along the horizontal axis in Fig. 6. At fixed M_t , varying

$$\alpha_s(M_Z) = 0.1180 \pm 0.00090 \quad (14)$$

gives the α_s uncertainties quoted above. The vertical bands in Fig. 6 are obtained by adding the intrinsic theory and α_s uncertainties linearly.

SusyHD was introduced in 2015 [66]. Its latest publicly distributed release, v1.0.2, remains the 2015 implementation. Our local v1.0.3 correction changes only the fast interpolation table and restores the missing g_3 dependence; it does not update the perturbative content or the uncertainty prescription of the original code. The agreement of its central prediction with **HSSUSY** at the level of about 0.5 GeV shows that the **SusyHD** central value remains a useful cross-check. However, its built-in uncertainty prescription is based on the perturbative information and uncertainty estimators implemented in 2015.

Since the release of **SusyHD**, substantial progress in high-scale SUSY Higgs mass calculations has been made. This includes improved EFT calculations, higher-order threshold corrections, improved treatment of the running SM parameters, and more systematic point-by-point estimates of missing higher-order effects [67, 68, 89, 101]. The **SusyHD** result

$$\Delta_{\text{th}} M_h^{\text{SusyHD}} \simeq 1.24 \text{ GeV} \quad (15)$$

should therefore be interpreted as a conservative legacy estimate associated with the 2015 **SusyHD** implementation. For the phenomenological interpretation, we adopt the more recent **HSSUSY** estimates,

$$\Delta_{\text{th}} M_h^{\text{HSSUSY}} = 0.482 \text{ GeV} \quad \text{and} \quad 0.471 \text{ GeV}, \quad (16)$$

for the bare and dynamically generated μ scenarios, respectively. These estimates remain prescription-dependent and should not be interpreted as statistical confidence intervals [89].

References

- [1] J. Martin, C. Ringeval, and V. Vennin, “Encyclopædia Inflationaris: Opiparous Edition,” *Phys. Dark Univ.* **5-6** (2014) 75–235, [arXiv:1303.3787](#) [[astro-ph.CO](#)].
- [2] K. D. Lozanov, “Lectures on Reheating after Inflation,” [arXiv:1907.04402](#) [[astro-ph.CO](#)].
- [3] J. Martin, C. Ringeval, and V. Vennin, “Cosmic Inflation at the crossroads,” *JCAP* **07** (2024) 087, [arXiv:2404.10647](#) [[astro-ph.CO](#)].
- [4] R. Kallosh and A. Linde, “On the Present Status of Inflationary Cosmology,” [arXiv:2505.13646](#) [[hep-th](#)].
- [5] F. L. Bezrukov and M. Shaposhnikov, “The Standard Model Higgs boson as the inflaton,” *Phys. Lett. B* **659** (2008) 703–706, [arXiv:0710.3755](#) [[hep-th](#)].
- [6] A. De Simone, M. P. Hertzberg, and F. Wilczek, “Running Inflation in the Standard Model,” *Phys. Lett. B* **678** (2009) 1–8, [arXiv:0812.4946](#) [[hep-ph](#)].
- [7] F. Bezrukov, A. Magnin, M. Shaposhnikov, and S. Sibiryakov, “Higgs inflation: consistency and generalisations,” *JHEP* **01** (2011) 016, [arXiv:1008.5157](#) [[hep-ph](#)].
- [8] M. P. Hertzberg, “Can Inflation be Connected to Low Energy Particle Physics?,” *JCAP* **08** (2012) 008, [arXiv:1110.5650](#) [[hep-ph](#)].
- [9] A. A. Starobinsky, “A new type of isotropic cosmological models without singularity,” *Phys. Lett. B* **91** no. 1, (1980) 99 – 102.
- [10] S. V. Ketov, “On the equivalence of Starobinsky and Higgs inflationary models in gravity and supergravity,” *J. Phys. A* **53** no. 8, (2020) 084001, [arXiv:1911.01008](#) [[hep-th](#)].
- [11] S. V. Ketov, “On Legacy of Starobinsky Inflation,” 1, 2025. [arXiv:2501.06451](#) [[gr-qc](#)].
- [12] S. J. Gates, M. T. Grisaru, M. Rocek, and W. Siegel, *Superspace Or One Thousand and One Lessons in Supersymmetry*, vol. 58 of *Frontiers in Physics*. 1983. [arXiv:hep-th/0108200](#).
- [13] J. Wess and J. Bagger, *Supersymmetry and supergravity*. Princeton University Press, Princeton, NJ, USA, 1992.
- [14] I. L. Buchbinder and S. M. Kuzenko, *Ideas and Methods of Supersymmetry and Supergravity or A Walk Through Superspace: A Walk Through Superspace*. Taylor & Francis, 1998.
- [15] **BICEP, Keck** Collaboration, P. A. R. Ade *et al.*, “Improved Constraints on Primordial Gravitational Waves using Planck, WMAP, and BICEP/Keck Observations through the 2018 Observing Season,” *Phys. Rev. Lett.* **127** no. 15, (2021) 151301, [arXiv:2110.00483](#) [[astro-ph.CO](#)].
- [16] A. Addazi, Y. Aldabergenov, and S. V. Ketov, “Curvature corrections to Starobinsky inflation can explain the ACT results,” *Phys. Lett. B* **869** (2025) 139883, [arXiv:2505.10305](#) [[gr-qc](#)].
- [17] **ACT** Collaboration, T. Louis *et al.*, “The Atacama Cosmology Telescope: DR6 Power Spectra, Likelihoods and Λ CDM Parameters,” [arXiv:2503.14452](#) [[astro-ph.CO](#)].

- [18] **ACT** Collaboration, E. Calabrese *et al.*, “The Atacama Cosmology Telescope: DR6 Constraints on Extended Cosmological Models,” [arXiv:2503.14454](#) [[astro-ph.CO](#)].
- [19] **SPT-3G** Collaboration, E. Camphuis *et al.*, “SPT-3G D1: CMB temperature and polarization power spectra and cosmology from 2019 and 2020 observations of the SPT-3G main field,” *Phys. Rev. D* **113** no. 8, (2026) 083504, [arXiv:2506.20707](#) [[astro-ph.CO](#)].
- [20] J. Ellis, D. V. Nanopoulos, K. A. Olive, and S. Verner, “A general classification of Starobinsky-like inflationary avatars of $SU(2,1)/SU(2) \times U(1)$ no-scale supergravity,” *JHEP* **03** (2019) 099, [arXiv:1812.02192](#) [[hep-th](#)].
- [21] Y. Ema, M. A. G. Garcia, W. Ke, K. A. Olive, and S. Verner, “Inflaton Decay in No-Scale Supergravity and Starobinsky-like Models,” *Universe* **10** no. 6, (2024) 239, [arXiv:2404.14545](#) [[hep-ph](#)].
- [22] I. Antoniadis, D. V. Nanopoulos, and K. A. Olive, “ R^2 -inflation derived from 4d strings, the role of the dilaton, and turning the Swampland into a mirage,” *JHEP* **06** (2025) 155, [arXiv:2410.16541](#) [[hep-th](#)].
- [23] J. Ellis, T. Gherghetta, K. Kaneta, W. Ke, and K. A. Olive, “Effects of radiative corrections on Starobinsky inflation,” *Phys. Rev. D* **112** no. 12, (2025) 123530, [arXiv:2510.15137](#) [[hep-ph](#)].
- [24] J. Ellis, T. Gherghetta, K. Kaneta, W. Ke, and K. A. Olive, “Radiative Corrections in Supergravity Models of Inflation,” [arXiv:2603.02389](#) [[hep-ph](#)].
- [25] S. Cecotti, “Higher derivative supergravity is equivalent to standard supergravity coupled to matter. 1.,” *Phys. Lett. B* **190** (1987) 86–92.
- [26] J. Gates, S. James and S. V. Ketov, “Superstring-inspired supergravity as the universal source of inflation and quintessence,” *Phys. Lett. B* **674** (2009) 59–63, [arXiv:0901.2467](#) [[hep-th](#)].
- [27] S. V. Ketov and A. A. Starobinsky, “Embedding $(R + R^2)$ -Inflation into Supergravity,” *Phys. Rev. D* **83** (2011) 063512, [arXiv:1011.0240](#) [[hep-th](#)].
- [28] F. Farakos, A. Kehagias, and A. Riotto, “On the Starobinsky Model of Inflation from Supergravity,” *Nucl. Phys. B* **876** (2013) 187–200, [arXiv:1307.1137](#) [[hep-th](#)].
- [29] S. V. Ketov and T. Terada, “Old-minimal supergravity models of inflation,” *JHEP* **12** (2013) 040, [arXiv:1309.7494](#) [[hep-th](#)].
- [30] A. Kehagias, A. Moradinezhad Dizgah, and A. Riotto, “Remarks on the Starobinsky model of inflation and its descendants,” *Phys. Rev. D* **89** no. 4, (2014) 043527, [arXiv:1312.1155](#) [[hep-th](#)].
- [31] A. Addazi and S. V. Ketov, “Energy conditions in Starobinsky supergravity,” *JCAP* **03** (2017) 061, [arXiv:1701.02450](#) [[hep-th](#)].
- [32] A. Hindawi, B. A. Ovrut, and D. Waldram, “Four-dimensional higher derivative supergravity and spontaneous supersymmetry breaking,” *Nucl. Phys. B* **476** (1996) 175–199, [arXiv:hep-th/9511223](#).
- [33] I. Dalianis, F. Farakos, A. Kehagias, A. Riotto, and R. von Unge, “Supersymmetry Breaking and Inflation from Higher Curvature Supergravity,” *JHEP* **01** (2015) 043, [arXiv:1409.8299](#) [[hep-th](#)].

- [34] M. B. Einhorn and D. R. T. Jones, “Inflation with Non-minimal Gravitational Couplings in Supergravity,” *JHEP* **03** (2010) 026, [arXiv:0912.2718 \[hep-ph\]](#).
- [35] K. Hamaguchi, T. Moroi, and T. Terada, “Complexified Starobinsky Inflation in Supergravity in the Light of Recent BICEP2 Result,” *Phys. Lett. B* **733** (2014) 305–308, [arXiv:1403.7521 \[hep-ph\]](#).
- [36] C. Pallis and N. Toumbas, “Starobinsky Inflation: From Non-SUSY To SUGRA Realizations,” *Adv. High Energy Phys.* **2017** (2017) 6759267, [arXiv:1612.09202 \[hep-ph\]](#).
- [37] E. Dudas, Y. Mambrini, and K. Olive, “Case for an EeV Gravitino,” *Phys. Rev. Lett.* **119** no. 5, (2017) 051801, [arXiv:1704.03008 \[hep-ph\]](#).
- [38] E. Dudas, T. Gherghetta, Y. Mambrini, and K. A. Olive, “Inflation and High-Scale Supersymmetry with an EeV Gravitino,” *Phys. Rev. D* **96** no. 11, (2017) 115032, [arXiv:1710.07341 \[hep-ph\]](#).
- [39] C. Pallis, “Gravity-mediated SUSY breaking, R symmetry, and hyperbolic Kähler geometry,” *Phys. Rev. D* **100** no. 5, (2019) 055013, [arXiv:1812.10284 \[hep-ph\]](#).
- [40] C. Pallis, “Inflection-point sgoldstino inflation in no-scale supergravity,” *Phys. Lett. B* **843** (2023) 138018, [arXiv:2302.12214 \[hep-ph\]](#).
- [41] D. S. Gorbunov and A. G. Panin, “Scalaron the mighty: producing dark matter and baryon asymmetry at reheating,” *Phys. Lett. B* **700** (2011) 157–162, [arXiv:1009.2448 \[hep-ph\]](#).
- [42] S. Ferrara, R. Kallosh, A. Linde, A. Marrani, and A. Van Proeyen, “Jordan Frame Supergravity and Inflation in NMSSM,” *Phys. Rev. D* **82** (2010) 045003, [arXiv:1004.0712 \[hep-th\]](#).
- [43] H. Jeong, K. Kamada, A. A. Starobinsky, and J. Yokoyama, “Reheating process in the R^2 inflationary model with the baryogenesis scenario,” *JCAP* **11** (2023) 023, [arXiv:2305.14273 \[hep-ph\]](#).
- [44] S. V. Ketov, “Inflationary cosmology from supergravity,” in *Handbook of Quantum Gravity*, C. Bambi, L. Modesto, and I. Shapiro, eds. Springer, Singapore, 2023. https://doi.org/10.1007/978-981-19-3079-9_51-1.
- [45] S. V. Ketov and N. Watanabe, “Cosmological properties of a generic \mathcal{R}^2 -supergravity,” *JCAP* **03** (2011) 011, [arXiv:1101.0450 \[hep-th\]](#).
- [46] S. V. Ketov, “Supergravity and Early Universe: the Meeting Point of Cosmology and High-Energy Physics,” *Int. J. Mod. Phys. A* **28** (2013) 1330021, [arXiv:1201.2239 \[hep-th\]](#).
- [47] S. V. Ketov and S. Tsujikawa, “Consistency of inflation and preheating in $F(R)$ supergravity,” *Phys. Rev. D* **86** (2012) 023529, [arXiv:1205.2918 \[hep-th\]](#).
- [48] S. V. Ketov, E. O. Pozdeeva, and S. Y. Vernov, “Inflation in $F(R)$ gravity models revisited after ACT,” *JCAP* **12** (2025) 040, [arXiv:2508.08927 \[gr-qc\]](#).
- [49] J.-O. Gong, S. V. Ketov, and T. Terada, “F-term multi-field inflation in supergravity without stabiliser superfields,” *JHEP* **12** (2025) 059, [arXiv:2508.20194 \[hep-th\]](#).
- [50] S. Toyama and S. V. Ketov, “Starobinsky inflation beyond the leading order,” *Phys. Rev. D* **110** no. 6, (2024) 063552, [arXiv:2407.21349 \[gr-qc\]](#).

- [51] D. S. Zharov, O. O. Sobol, and S. I. Vilchinskii, “ACT observations, reheating, and Starobinsky and Higgs inflation,” *Phys. Rev. D* **112** no. 2, (2025) 023544, [arXiv:2505.01129 \[astro-ph.CO\]](#).
- [52] **Planck** Collaboration, Y. Akrami *et al.*, “Planck 2018 results. X. Constraints on inflation,” *Astron. Astrophys.* **641** (2020) A10, [arXiv:1807.06211 \[astro-ph.CO\]](#).
- [53] E. G. M. Ferreira, E. McDonough, L. Balkenhol, R. Kallosh, L. Knox, and A. Linde, “BAO-CMB tension and implications for inflation,” *Phys. Rev. D* **113** no. 4, (2026) 043524, [arXiv:2507.12459 \[astro-ph.CO\]](#).
- [54] D. Frolovsky and S. V. Ketov, “Are single-field models of inflation and PBHs production ruled out by ACT observations?,” *Mod. Phys. Lett. A* **40** no. 40, (2025) 2550182, [arXiv:2505.17514 \[astro-ph.CO\]](#).
- [55] P. Candelas and S. Kalara, “Yukawa Couplings for a Three Generation Superstring Compactification,” *Nucl. Phys. B* **298** (1988) 357–368.
- [56] A. Font, L. E. Ibanez, H. P. Nilles, and F. Quevedo, “Yukawa Couplings in Degenerate Orbifolds: Towards a Realistic $SU(3) \times SU(2) \times U(1)$ Superstring,” *Phys. Lett. B* **210** (1988) 101. [Erratum: *Phys.Lett.B* 213, 564 (1988)].
- [57] A. Cheshel and S. V. Ketov, “IIA string instanton corrections to the four fermion correlator in the intersection of Del Pezzo surfaces,” *Phys. Rev. D* **67** (2003) 026007, [arXiv:hep-th/0209063](#).
- [58] I. J. R. Aitchison, “Supersymmetry and the MSSM: An Elementary introduction,” [arXiv:hep-ph/0505105](#).
- [59] J. E. Kim and H. P. Nilles, “The mu Problem and the Strong CP Problem,” *Phys. Lett. B* **138** (1984) 150–154.
- [60] U. Ellwanger, C. Hugonie, and A. M. Teixeira, “The Next-to-Minimal Supersymmetric Standard Model,” *Phys. Rept.* **496** (2010) 1–77, [arXiv:0910.1785 \[hep-ph\]](#).
- [61] G. F. Giudice and A. Masiero, “A Natural Solution to the mu Problem in Supergravity Theories,” *Phys. Lett. B* **206** (1988) 480–484.
- [62] J. A. Casas and C. Munoz, “A Natural solution to the mu problem,” *Phys. Lett. B* **306** (1993) 288–294, [arXiv:hep-ph/9302227](#).
- [63] K. J. Bae, H. Baer, V. Barger, and D. Sengupta, “Revisiting the SUSY μ problem and its solutions in the LHC era,” *Phys. Rev. D* **99** no. 11, (2019) 115027, [arXiv:1902.10748 \[hep-ph\]](#).
- [64] A. Brignole, L. E. Ibanez, and C. Munoz, “Soft supersymmetry breaking terms from supergravity and superstring models,” *Adv. Ser. Direct. High Energy Phys.* **18** (1998) 125–148, [arXiv:hep-ph/9707209](#).
- [65] A. Brignole, L. E. Ibanez, and C. Munoz, “Soft supersymmetry breaking terms from supergravity and superstring models,” *Adv. Ser. Direct. High Energy Phys.* **21** (2010) 244–268.
- [66] J. Pardo Vega and G. Villadoro, “SusyHD: Higgs mass Determination in Supersymmetry,” *JHEP* **07** (2015) 159, [arXiv:1504.05200 \[hep-ph\]](#).

- [67] P. Athron, J.-h. Park, T. Steudtner, D. Stockinger, and A. Voigt, “Precise Higgs mass calculations in (non-)minimal supersymmetry at both high and low scales,” *JHEP* **01** (2017) 079, [arXiv:1609.00371 \[hep-ph\]](#).
- [68] P. Athron *et al.*, “FlexibleSUSY 2.0: Extensions to investigate the phenomenology of SUSY and non-SUSY models,” *Comput. Phys. Commun.* **230** (2018) 145–217, [arXiv:1710.03760 \[hep-ph\]](#).
- [69] B. C. Allanach and A. Voigt, “Uncertainties in the Lightest CP Even Higgs Boson Mass Prediction in the Minimal Supersymmetric Standard Model: Fixed Order Versus Effective Field Theory Prediction,” *Eur. Phys. J. C* **78** no. 7, (2018) 573, [arXiv:1804.09410 \[hep-ph\]](#).
- [70] E. Bagnaschi, G. F. Giudice, P. Slavich, and A. Strumia, “Higgs Mass and Unnatural Supersymmetry,” *JHEP* **09** (2014) 092, [arXiv:1407.4081 \[hep-ph\]](#).
- [71] **ATLAS** Collaboration, “Search for long-lived charginos based on a disappearing-track signature using 136 fb^{-1} of pp collisions at $\sqrt{s} = 13 \text{ TeV}$ with the ATLAS detector,” *Eur. Phys. J. C* **82** no. 7, (2022) 606, [arXiv:2201.02472 \[hep-ex\]](#).
- [72] G. F. Giudice, M. A. Luty, H. Murayama, and R. Rattazzi, “Gaugino mass without singlets,” *JHEP* **12** (1998) 027, [arXiv:hep-ph/9810442](#).
- [73] T. Moroi and L. Randall, “Wino cold dark matter from anomaly mediated SUSY breaking,” *Nucl. Phys. B* **570** (2000) 455–472, [arXiv:hep-ph/9906527](#).
- [74] M. Ibe, R. Kitano, H. Murayama, and T. Yanagida, “Viable supersymmetry and leptogenesis with anomaly mediation,” *Phys. Rev. D* **70** (2004) 075012, [arXiv:hep-ph/0403198](#).
- [75] E. W. Kolb and A. J. Long, “Cosmological gravitational particle production and its implications for cosmological relics,” *Rev. Mod. Phys.* **96** no. 4, (2024) 045005, [arXiv:2312.09042 \[astro-ph.CO\]](#).
- [76] Y. Ema, K. Nakayama, and Y. Tang, “Production of Purely Gravitational Dark Matter,” *JHEP* **09** (2018) 135, [arXiv:1804.07471 \[hep-ph\]](#).
- [77] J. Hisano, S. Matsumoto, M. Nagai, O. Saito, and M. Senami, “Non-perturbative effect on thermal relic abundance of dark matter,” *Phys. Lett. B* **646** (2007) 34–38, [arXiv:hep-ph/0610249](#).
- [78] A. Hryczuk, R. Iengo, and P. Ullio, “Relic densities including Sommerfeld enhancements in the MSSM,” *JHEP* **03** (2011) 069, [arXiv:1010.2172 \[hep-ph\]](#).
- [79] M. Beneke, C. Hellmann, and P. Ruiz-Femenia, “Heavy neutralino relic abundance with Sommerfeld enhancements - a study of pMSSM scenarios,” *JHEP* **03** (2015) 162, [arXiv:1411.6930 \[hep-ph\]](#).
- [80] M. Beneke, A. Bharucha, F. Dighera, C. Hellmann, A. Hryczuk, S. Recksiegel, and P. Ruiz-Femenia, “Relic density of wino-like dark matter in the MSSM,” *JHEP* **03** (2016) 119, [arXiv:1601.04718 \[hep-ph\]](#).
- [81] M. Beneke, R. Szafron, and K. Urban, “Sommerfeld-corrected relic abundance of wino dark matter with NLO electroweak potentials,” *JHEP* **02** (2021) 020, [arXiv:2009.00640 \[hep-ph\]](#).

- [82] J. Hisano, S. Matsumoto, M. M. Nojiri, and O. Saito, “Direct Detection of the Wino- and Higgsino-like Neutralino Dark Matters at One-Loop Level,” *Phys. Rev. D* **71** (2005) 015007, [arXiv:hep-ph/0407168](#).
- [83] J. Hisano, K. Ishiwata, and N. Nagata, “Gluon contribution to the dark matter direct detection,” *Phys. Rev. D* **82** (2010) 115007, [arXiv:1007.2601 \[hep-ph\]](#).
- [84] J. Hisano, K. Ishiwata, and N. Nagata, “QCD effects on direct detection of wino dark matter,” *JHEP* **06** (2015) 097, [arXiv:1504.00915 \[hep-ph\]](#).
- [85] **LUX-ZEPLIN** Collaboration, J. Aalbers *et al.*, “Dark Matter Search Results from 4.2 Tonne-Years of Exposure of the LUX-ZEPLIN (LZ) Experiment,” [arXiv:2410.17036 \[hep-ex\]](#).
- [86] D. S. Akerib *et al.*, “The XLZD Design Book: Towards the Next-Generation Liquid Xenon Observatory for Dark Matter and Neutrino Physics,” [arXiv:2410.17137 \[physics.ins-det\]](#).
- [87] J. Aalbers *et al.*, “DARWIN: towards the ultimate dark matter detector,” *JCAP* **11** (2016) 017, [arXiv:1606.07001 \[astro-ph.IM\]](#).
- [88] **Particle Data Group** Collaboration, S. Navas *et al.*, “Review of particle physics,” *Phys. Rev. D* **110** no. 3, (2024) 030001.
- [89] P. Slavich *et al.*, “Higgs-mass predictions in the MSSM and beyond,” *Eur. Phys. J. C* **81** no. 5, (2021) 450, [arXiv:2012.15629 \[hep-ph\]](#).
- [90] M. Ibe, S. Matsumoto, and R. Sato, “Mass Splitting between Charged and Neutral Winos at Two-Loop Level,” *Phys. Lett. B* **721** (2013) 252–260, [arXiv:1212.5989 \[hep-ph\]](#).
- [91] **ATLAS** Collaboration, “Search for long-lived charginos and τ -sleptons using final states with a disappearing track in pp collisions at $\sqrt{s} = 13$ TeV with the ATLAS detector,” [arXiv:2603.08315 \[hep-ex\]](#).
- [92] **ATLAS** Collaboration, “ATLAS sensitivity to winos and higgsinos with a highly compressed mass spectrum at the HL-LHC,” tech. rep., CERN, 2018. <https://cds.cern.ch/record/2647294>.
- [93] ATLAS and CMS Collaborations, “Highlights of the HL-LHC physics projections by ATLAS and CMS,” [arXiv:2504.00672 \[hep-ex\]](#).
- [94] CMS Collaboration, “Projections for top quark mass measurements at the HL-LHC,” CMS Note CMS-NOTE-2025-002, CERN, 2025.
- [95] M. Saito, R. Sawada, K. Terashi, and S. Asai, “Discovery reach for wino and higgsino dark matter with a disappearing track signature at a 100 TeV pp collider,” *Eur. Phys. J. C* **79** no. 6, (2019) 469, [arXiv:1901.02987 \[hep-ph\]](#).
- [96] N. Arkani-Hamed, S. Dimopoulos, G. F. Giudice, and A. Romanino, “Aspects of split supersymmetry,” *Nucl. Phys. B* **709** (2005) 3–46, [arXiv:hep-ph/0409232](#).
- [97] Y. Aldabergenov, A. Addazi, and S. V. Ketov, “Primordial black holes from modified supergravity,” *Eur. Phys. J. C* **80** no. 10, (2020) 917, [arXiv:2006.16641 \[hep-th\]](#).
- [98] Y. Aldabergenov, A. Addazi, and S. V. Ketov, “Testing Primordial Black Holes as Dark Matter in Supergravity from Gravitational Waves,” *Phys. Lett. B* **814** (2021) 136069, [arXiv:2008.10476 \[hep-th\]](#).

- [99] G. Senjanovic, “See-saw and grand unification,” 2005. [arXiv:hep-ph/0501244 \[hep-ph\]](#).
- [100] F. J. de Anda, S. F. King, and E. Perdomo, “ $SO(10) \times S_4$ Grand Unified Theory of Flavour and Leptogenesis,” *JHEP* **12** (2017) 075, [arXiv:1710.03229 \[hep-ph\]](#).
- [101] E. Bagnaschi, J. Pardo Vega, and P. Slavich, “Improved determination of the Higgs mass in the MSSM with heavy superpartners,” *Eur. Phys. J. C* **77** no. 5, (2017) 334, [arXiv:1703.08166 \[hep-ph\]](#).